The Canadian Mineralogist
Vol. 38, pp. 951-974 (2000)

POST-ACCRETION MAGMATISM WITHIN THE KUIU–ETOLIN IGNEOUS BELT, SOUTHEASTERN ALASKA

JENNIFER LINDLINE§

Natural Resources Management Program, New Mexico Highlands University, Las Vegas, New Mexico 87701, U.S.A.

WILLIAM A. CRAWFORD AND MARIA LUISA CRAWFORD

Department of Geology, Bryn Mawr College, Bryn Mawr, Pennsylvania 19010, U.S.A.

GOMAA I. OMAR

Department of Earth and Environmental Sciences, University of Pennsylvania, Philadelphia, Pennsylvania 19104, U.S.A.

ABSTRACT

Petrological and geochronological studies of Tertiary granite and gabbro plutons in southeastern Alaska provide information about the Mid-Miocene post-accretionary magmatic history of the region. The Burnett Inlet Igneous Complex is a 20 Ma bimodal granite–gabbro complex located on Etolin Island and adjacent areas in central southeastern Alaska. It consists of three main members: granite, alkali granite, and a gabbro–diorite unit consisting of intermingled mafic, hybrid and granitic rocks. Mafic magmatic enclaves are ubiquitous in the complex. They occur as isolated inclusions in the silicic plutons and as packed masses in the intermingled zones of the gabbro–diorite unit. The mafic enclaves typically display round and pillow-like shapes, igneous textures, and chilled margins, and thus denote the mingling of mafic and felsic magmas. Petrographic and geochemical features indicate that the complex developed *via* a combination of fractional crystallization, crystal accumulation and magma mixing. Systematic changes in mineralogy and coherent, curvilinear trends on geochemical diagrams indicate that the mafic and felsic magmas each evolved separately, mainly by crystal accumulation and fractionation. Magma-mixing textures, such as micro-inclusions and quartz xenocrysts in some mafic rocks, suggest mafic–felsic magma mixing and hybridization. However, the compositional and viscosity differences precluded bulk mixing between end-member granite and basalt magmas. Mixing probably involved intermediate magmas, whose smaller differences in composition and viscosity would have permitted hybridization. Both the mafic and felsic units have within-plate geochemical characteristics, indicating that post-accretionary magmatism occurred within an overall extensional tectonic setting. Distributions of apatite fission-track lengths and mineral-cooling curves imply that the magmatic rocks cooled to less than 100°C within 5 million years of emplacement. The complex is interpreted to have initially evolved as a shallow-level silicic magma chamber heated by underplated basaltic magma derived from partial melting of enriched upper mantle. Subsequent invasion of the silicic magma chamber by basaltic intrusions induced an explosive eruption phase, followed by rapid crystallization and cooling of the entire complex.

Keywords: Kuiu–Etolin Igneous Belt, enclave, fractional crystallization, within-plate basalt, magma mixing, A-type granite, Alaska.

SOMMAIRE

Les études pétrologiques et géochronologiques de plutons de granite et de gabbro d'âge tertiaire dans le sud-est de l'Alaska fournissent des indices à propos de l'évolution magmatique suite à l'accrétion dans la région au miocène moyen. Le complexe igné bimodal (granite–gabbro) de Burnett Inlet, mis en place il y a 20 million d'années, est situé sur l'île d'Etolin et dans les régions avoisinantes de la partie centrale du sud-est de l'Alaska. Nous distinguons trois membres principaux: granite, granite alcalin, et une unité mixte de gabbro–diorite contenant un mélange de roches mafiques, hybrides et granitiques. Les enclaves mafiques sont très répandues dans ce complexe. Elles se trouvent en isolation dans les plutons siliceux et en empilements compacts dans les zones mixtes de l'unité de gabbro–diorite. Les enclaves mafiques font preuve de formes rondes ou en coussin, des textures ignées et des bordures figées, démontrant ainsi l'importance d'un mélange de magmas mafique et felsique. Les caractéristiques pétrographiques et géochimiques indiquent que le complexe se développa grâce à une combinaison de cristallisation fractionnée, d'une accumulation de cristaux, et d'un mélange de magmas. Des changements systématiques en minéralogie et des tracés cohérents et courbes sur des diagrammes de données géochimiques indiquent que les magmas mafique

§ *E-mail address*: jlindline@hotmail.com

et felsique ont évolué séparément, surtout par accumulation de cristaux et par fractionnement. Des textures typiques de mélange de magmas, par exemple des micro-inclusions et des xénocristaux de quartz dans certaines roches mafiques, témoignent d'un mélange de magmas et d'une hybridisation. Toutefois, les différences en composition et en viscosité excluent la possibilité d'un mélange complet entre deux magmas, l'un granitique et l'autre basaltique. Le processus de mélange aurait plutôt impliqué des magmas intermédiaires, dont les différences moins grandes en composition et en viscosité auraient favorisé l'hybridisation. Les roches des unités felsiques et mafiques possèdent des caractéristiques d'un magmatisme intra-plaques, témoignant d'une activité post-accrétion dans un milieu extensionnel. La distribution de tracés de fission de l'apatite et les courbes de refroidissement des minéraux montrent que ces roches magmatiques ont refroidi à moins de 100°C dans l'espace de cinq million d'années après leur mise en place. Le complexe aurait d'abord été réchauffé par dessous par la venue de magma basaltique dérivé par fusion partielle du manteau supérieur enrichi. Par la suite, l'introduction de venues basaltiques dans la chambre magmatique occupée par le magma siliceux aurait provoqué une phase explosive d'éruption, et ensuite une cristallisation rapide et un refroidissement complet du complexe.

(Traduit par la Rédaction)

Mots-clés: ceinture ignée de Kuiu–Etolin, enclave, cristallisation fractionnée, basalte intra-plaques, mélange de magmas, granite de type A, Alaska.

Introduction

Granitic rocks are found in nearly all plate tectonic environments, yet the vast majority are located in those orogenic regions (ocean–continent and continent–continent collision zones) where the ponding of subduction-related basalt or thickening of the crust has increased the temperature of crustal rocks to that of melting. Anorogenic granites, less abundant than orogenic granites, are typically associated with rifting of the continental crust (*e.g.*, Bockelie 1978, Gilbert 1983, Gilbert & Donovan 1982), aborted rifting events (Lameyre & Bowden 1982, Black & Girod 1970) and possibly hot-spot activity (Maniar & Piccoli 1989). They commonly are explained by underplating of the crust by mantle-derived basalt generated *via* extensional tectonics or as a result of a mantle plume.

A northwesterly trending field approximately 170 km long of silicic volcanic and plutonic rocks of Miocene age outcrops along the coast of southeastern Alaska. This belt, named the Kuiu–Etolin igneous belt by Brew *et al*. (1979, 1981), consists of post-terrane accretion granitic plutons, many of which have the mineralogical and geochemical features of anorogenic granite described by Clemens *et al*. (1986). Numerous granites of the Kuiu–Etolin igneous belt have relatively alkaline and metaluminous compositions, are typically Ca-poor, and contain high amounts of Zr, Nb, Y, the rare-earth elements (*REE*) and Zn, and low amounts of Ni and Cr. Previous geological and petrological studies of these Miocene igneous rocks have focused on their distribution, mineral content, and economic potential (Brew *et al*. 1979, Hunt 1984, Douglass *et al.* 1989, Lindline 1993), but their origin and evolution have remained poorly understood. To address these issues and to help interpret the Middle Tertiary magmatic history of southeastern Alaska, we studied the collection of plutons that make up the Burnett Inlet Igneous Complex located in the southern part of the Kuiu–Etolin Igneous Belt, approximately 80 kilometers north of Ketchikan (Fig. 1). The complex, unlike other plutons of the Kuiu–Etolin igneous belt, is a bimodal suite comprising alkali feldspar granite, granite and gabbro. Field relationships, petrographic features, and geochemical characteristics indicate that the complex is composed of physically and chemically distinct but contemporaneous granite and gabbro bodies. This conclusion differs from previous interpretations (basalt differentiation series, Hunt 1984; migmatite complex, Brew *et al.* 1984).

Mafic magmatic enclaves are common features of the granitic plutons and granitic dikes within the complex. The enclaves demonstrate a mingling relationship between mafic and felsic magmas and possibly represent the vestiges of mafic igneous activity that initiated anorogenic granite magmatism in this area. We conclude that the complex evolved from the combined effects of fractional crystallization, crystal accumulation and mixing of mafic and felsic magmas. Fractional crystallization and crystal accumulation processes in both the mafic and felsic suites are shown by the systematic change in major mineral phases and coherent, curvilinear trends on most major- and trace-element diagrams. Magma mixing and hybridization are indicated by disequilibrium textures, incongruous trends of some elements (Ba, Zr, Y), and the elevated initial strontium ratio of mafic magmatic rocks (on average, 0.7046). Our geochronological evidence, including apatite fission-track age data and horizontal patterns of confined track-length distribution, documents the rapid cooling of the complex. Finally, we suggest that continued injection of mafic magma triggered eruption of the shallow crustal magma chamber that contained these igneous units.

Geology of the Study Area

The geological history of southeastern Alaska from the middle Jurassic through the Eocene was marked by the accretion of tectonostratigraphic terranes to western North America (Coney *et al.* 1980, Jones *et al.* 1981, Monger *et al.* 1982, Coney & Jones 1985). Numerous

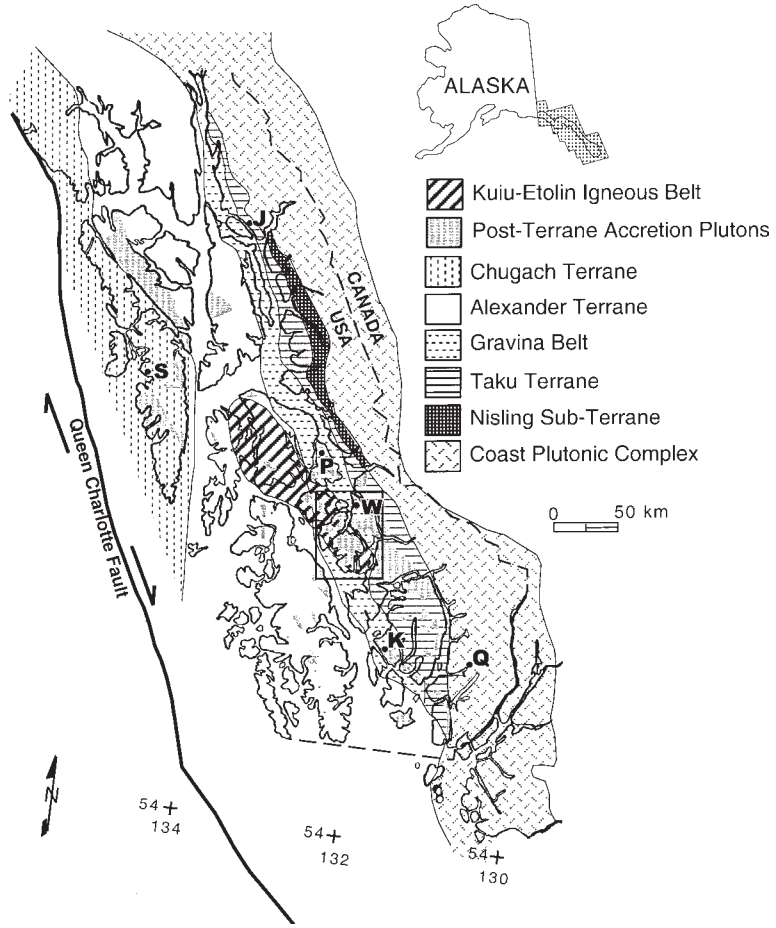

FIG. 1. Map of lithotectonic units in southeastern Alaska after Wheeler *et al.* (1991) and location of the Kuiu–Etolin magmatic belt (Brew 1994, Brew & Morrell 1983, Brew *et al.* 1984). A box encloses the Burnett Inlet Igneous Complex. Larger towns and features are noted (K: Ketchikan, W: Wrangell, P: Petersburg, S: Sitka, J: Juneau, Q: Quartz Hill).

100–90 Ma calc- alkaline bodies of foliated garnet- and epidote-bearing plagioclase porphyritic quartz diorite, tonalite and granodiorite occur throughout the region and represent the deeply eroded remnants of a mid-Cretaceous magmatic arc. Significant melting events continued to affect the region and resulted in the emplacement of the Coast Mountains Batholith from latest Cretaceous to Eocene (75–55 Ma; Gehrels *et al.* 1991). The batholith contains a variety of intrusive rocks, many of which resulted from subduction-related magmatism (Barker & Arth 1990). Following approximately 35 million years of igneous inactivity, post-accretionary magmatism and subsequent metamorphism of the country rocks affected a large part of the region. The Middle Miocene Kuiu–Etolin Igneous Belt is a discontinuous tract of predominantly silicic volcanic and plutonic rocks that cross-cuts the tectonostratigraphic terrane boundaries established during the Mesozoic accretionary events (Fig. 1). Numerous smaller igneous bodies, including molybdenite-bearing rocks at Quartz Hill (115 km east of Ketchikan), also were emplaced at this time.

The 20 Ma Burnett Inlet Igneous Complex (Fig. 2) is a member of the Kuiu–Etolin Igneous Belt and the focus of this study. The complex intruded fine-grained black biotite-grade schist correlated with the marine flysch sediments and interlayered volcanic rocks of the Gravina–Nutzotin belt of Jurassic–Cretaceous age, more

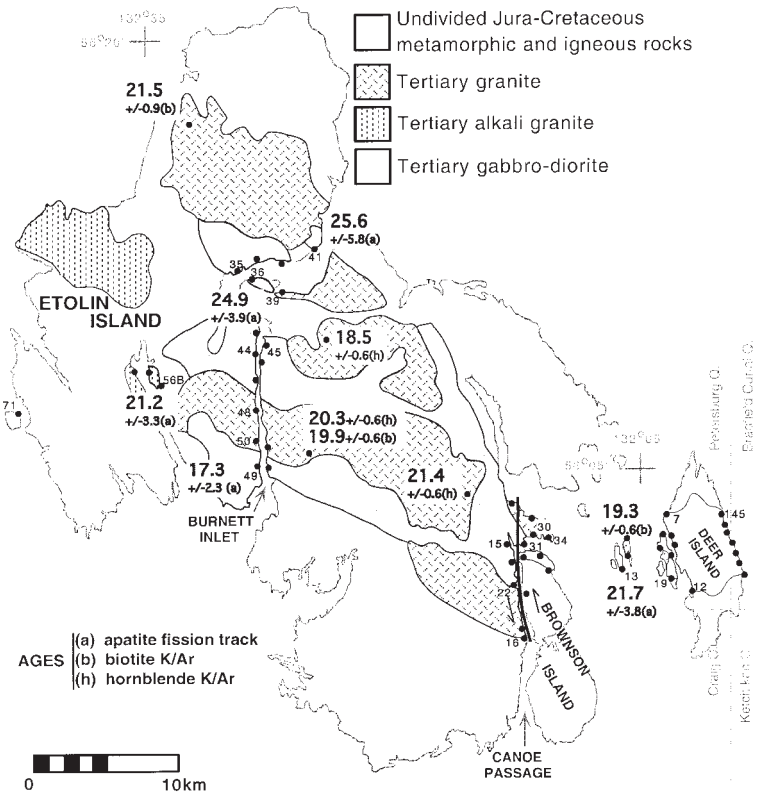

FIG. 2. Simplified geological map of the study area after Brew *et al.* (1984). Map shows all sample and data-collecting localities (•); numbers refer to samples listed in Tables 1 and 2 and in Figure 5. Large numbers are radiogenic ages in million years from the indicated geochronometers.

specifically the Seymour Canal Formation (Berg *et al.* 1972, Brew *et al.* 1984). Contacts with the metamorphic rocks are straight, sharp and discordant. Metamorphic pendants and xenoliths are common throughout. Minor occurrences of alluvium, colluvium and tidal mudflats and some glaciofluvial deposits overlie the major geological units. Brecciated rocks along the eastern side of Canoe Passage (Fig. 2) mark the trace of a Miocene (or younger) high-angle strike-slip fault (Koch *et al.* 1977). Northeast- and north-northwest-trending nearly vertical mafic dikes cross-cut the complex and neighboring rocks. These dikes are likely related to the regional swarm of mafic dikes that have been mapped throughout southeastern Alaska and coastal British Columbia (Smith 1973, Lull & Plafker 1988). Although radiometric ages are not available for these mafic dikes, they are relatively younger than the 20 Ma granite–gabbro complex they intrude as they were emplaced after the intrusions cooled sufficiently to support fracturing.

The Burnett Inlet Igneous Complex consists of three main plutonic units: granite, alkali feldspar granite, and gabbro–diorite. The granite and alkali granite are massive and homogeneous in both texture and composition. These medium- to coarse-grained euhedral equigranular to seriate-textured felsic rocks are characterized by abundant miarolitic cavities and graphic intergrowths. The heterogeneous gabbro–diorite unit can be subdivided into three lithological types: mafic plutonic rock, mafic magmatic enclaves, and hybrid rocks. The uniform gabbro–diorite displays a generally massive medium- to coarse-grained subhedral equigranular texture. In some places, variations in the proportions of mafic minerals and plagioclase on the scale of 1 to 2 cm define a weak, west–northwest-trending moderately dipping layering. The composite zones range from meter-wide dikes to several meter-wide areas of intermingled mafic and felsic igneous rock (Fig. 3). In the composite zones, the mafic rocks, herein termed enclaves, commonly are rounded and lobate, and appear

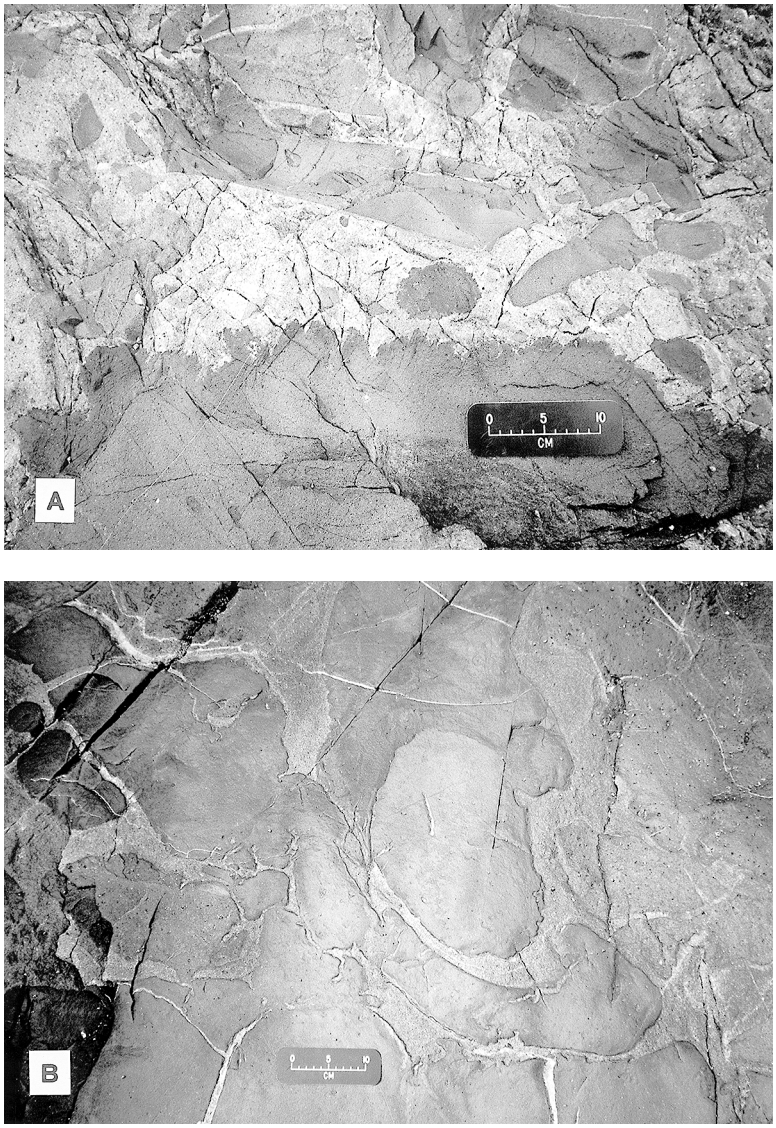

FIG. 3. A. Outcrop view of abundant mafic magmatic enclaves in granite, southwestern Burnett Inlet. Note various sizes and shapes of enclaves and the serrated edge of lower enclave. B. Pillow-like mafic magmatic enclaves with intervening leucocratic material from within gabbro unit, southeast Deer Island.

similar to submarine pillow basalt. These plutonic "pillows" vary greatly in size and dimension, from small and nearly equant (1 cm by 1 cm) to large and elongate (up to 2 m by 4 m). Enclave margins are typically sharp, fine-grained, and scalloped or serrated. These enclave characteristics have been described in many plutons and indicate the commingling of mafic and felsic magmas (*e.g.*, Didier 1973, Vernon 1984, Barbarin 1988). The felsic rocks of the composite zones range from granite to granodiorite and have higher amounts of biotite and hornblende than the enclave-free granitic rocks. Hybrid rocks contain highly disaggregated enclaves and microinclusions set in a dioritic to granodioritic matrix. The hybrid rocks show a range of grain sizes and concentrations of mafic minerals 0.1 to 2.0 cm across. Centimeter-scale heterogeneities in mineralogy and grain size

suggest that the hybrid rocks are the products of physical mixing of mafic and felsic magmas.

Analytical Techniques

One hundred samples were chosen for thin-section study. Rock names are based on both modal and visual estimations of mineral abundances and follow IUGS recommendations (Streckeisen 1978). Enclave-free rocks were sampled approximately 5 m from commingled zones. The felsic portions of host–enclave pairs were sampled at least 10 cm from analyzed enclaves. Approximately 1 kg samples were collected from surface outcrops. Samples were slabbed, cleared of weathered pieces, reduced to fine grains in a jaw crusher, and pulverized to a powder in a ceramic puck mill. Concentrations of most major elements were determined by XRAL Laboratories using X-ray fluorescence spectroscopy. The compositions of underscored samples in Table 1 were determined by direct current plasma –

TABLE 1. WHOLE-ROCK GEOCHEMISTRY AND MODAL DATA FOR REPRESENTATIVE SAMPLES OF THE BURNETT INLET IGNEOUS COMPLEX, SOUTHEASTERN ALASKA

	87145	9219	9222	92341	9216	9230	9239	9244	9245	927h	9215h	92352h	92351	927e	9215e	92352e	9244e	9271
	gd	gd	gd	gd	g	a	g	a	g	f	f	f	hy	e	e	e	e	gr
Pl vol.%	46	61	61	55	38	8	38	28	40	37	44	12	17	41	42	19	3	clasts
Qtz	tr	1	tr	6	38	27	34	36	13	35	32	23	29	3	10	30	30	clasts
Or	nd	nd	nd	nd	12	63	18	33	12	27	6	62	39	4	7	3	58	clasts
Bt	2	2	3	11	10	tr	7	tr	8	2	16	2	4	19	16	16	tr	tr
Hbl	3	tr	13	8	2	1	2	2	22	tr	tr	1	8	28	16	2	8	nd
Cpx	19	2	8	8	nd	nd	nd	nd	2	nd	nd	nd	4	3	10	5	nd	nd
Opx	tr	15	12	5	nd	nd	nd	nd	nd	nd	nd	nd	tr	tr	tr	25	nd	nd
Ol	5	1	nd	nd	nd	nd	nd	nd	nd	nd	nd	nd	tr	nd	nd	nd	nd	nd
Mgt-Ilm	2	2	tr	1	tr	tr	tr	tr	3	tr	1	tr	1	2	tr	tr	tr	2
Chl	6	2	1	5	tr	tr	tr	tr	nd	tr	1	nd	nd	tr	nd	nd	nd	tr
Ap	tr	tr	2	tr	tr	tr	tr	tr	tr	tr	tr	tr	tr	tr	tr	tr	tr	nd
Zrn	nd	nd	nd	nd	tr	tr	tr	tr	nd	tr	tr	tr	nd	nd	nd	nd	nd	nd
Ttn	tr	tr	tr	tr	tr	nd	nd	1	nd	nd	nd	nd	tr	nd	nd	nd	nd	nd
**	18	15	nd	2	tr	tr	1	tr	tr	tr	tr	tr	tr	tr	tr	tr	tr	tr
SiO_2 wt.%	48.80	49.90	48.70	53.80	72.60	72.45	68.47	74.45	63.25	74.30	75.42	70.35	64.90	49.80	56.79	58.44	68.80	41.00
TiO_2	0.56	1.08	0.87	1.07	0.21	0.19	0.44	0.20	0.79	0.09	0.24	0.32	0.65	1.22	1.17	1.12	0.32	0.94
Al_2O_3	15.40	15.90	16.90	16.20	13.30	13.85	16.36	12.92	16.24	13.10	14.26	14.10	14.20	16.30	16.32	16.30	13.50	16.40
Fe_2O_{3T}	10.00	9.15	9.09	8.58	1.89	2.07	3.05	2.70	5.25	1.08	1.79	3.28	5.30	9.20	7.62	7.36	3.79	12.70
MgO	9.59	7.36	8.06	4.35	0.39	0.20	1.21	0.10	1.74	0.11	0.61	0.58	1.82	6.42	4.98	2.80	0.50	3.34
MnO	0.16	0.14	0.13	0.13	0.04	0.02	0.07	0.04	0.11	0.01	0.01	0.06	0.07	0.14	0.16	0.12	0.08	1.99
CaO	9.33	8.43	9.55	7.55	1.19	0.82	2.99	0.66	3.62	0.67	2.84	1.59	3.22	8.33	8.64	5.52	1.46	9.57
Na_2O	2.05	2.99	2.49	3.22	3.44	3.96	3.98	4.08	4.63	3.54	3.52	3.87	3.59	3.24	3.45	4.51	4.59	2.18
K_2O	0.40	0.87	0.77	1.40	4.84	5.20	3.48	4.58	3.08	5.22	2.58	4.94	3.71	1.30	1.60	2.85	4.78	1.07
P_2O_5	0.14	0.31	0.12	0.24	0.05	0.03	n.d.	n.d.	n.d.	0.01	n.d.	n.d.	0.13	0.37	n.d.	n.d.	0.07	1.43
LOI	0.90	1.50	1.10	1.65	0.40	0.28	0.20	0.31	0.86	0.05	0.51	0.48	0.50	1.35	0.90	0.41	0.50	8.80
SUM	97.33	97.63	97.78	98.19	98.35	99.07	100.25	100.04	99.57	98.18	101.78	99.57	98.09	97.67	101.63	99.43	98.39	99.42
Cr ppm	343.7	223.4	337.0	58.5	6.5	21.9	8.8	9.4	10.4	20.7	15.3	12.9	35.8	180.1	425.1	39.0	10.5	27.3
Co	30.2	26.7	42.7	24.5	1.8	1.0	5.9	0.9	1.3	1.1	4.2	3.4	10.8	27.5	28.3	15.4	2.4	34.1
Ni	92.8	97.7	83.2	10.8	13.1	25.4	15.7	17.5	10.5	59.5	6.9	14.0	116.3	40.8	14.3	28.9	14.5	29.9
Rb	4.4	13.1	24.9	40.8	148.8	149.1	98.4	143.4	105.7	130.9	46.8	120.6	106.4	28.5	39.5	42.3	152.6	21.9
Sr	533.3	599.0	430.8	446.6	116.2	78.6	426.8	45.3	81.8	34.8	239.4	95.7	188.2	507.0	292.8	403.0	27.2	547.4
Y	10.8	17.7	15.4	25.9	24.8	30.1	14.9	62.0	36.4	41.0	6.5	46.4	56.1	27.6	27.8	30.8	65.9	40.3
Zr	42.7	124.1	79.3	113.8	122.0	207.5	109.9	455.1	258.4	108.4	144.0	324.4	366.3	135.6	139.6	309.8	168.5	72.8
Nb	3.1	11.9	11.2	10.0	13.3	13.1	15.6	46.0	13.9	15.6	4.1	21.7	21.3	15.3	7.0	19.0	49.9	5.7
Ba	200.9	373.6	309.5	488.8	627.0	1087	797.4	375.3	1246	132.8	1008	442.6	311.2	462.9	488.7	988.2	188.3	494.0
La	7.1	18.0	9.6	19.5	29.9	41.9	35.5	57.9	46.7	42.1	17.6	45.5	34.4	24.3	16.4	33.7	24.7	28.6
Ce	15.0	37.3	18.0	35.1	50.0	68.2	54.8	99.7	76.7	73.9	22.9	77.6	70.5	45.2	30.6	59.0	51.5	58.0
Pr	1.9	4.6	2.7	4.3	5.6	7.7	5.7	11.3	8.5	8.4	2.2	8.7	6.6	5.7	3.9	7.2	7.0	6.6
Nd	8.8	20.4	10.3	17.6	20.3	27.6	20.2	42.8	31.2	30.3	7.3	32.4	25.0	23.6	17.1	28.8	29.5	31.6
Sm	1.9	3.6	2.4	4.5	4.4	5.8	3.5	9.1	7.9	7.1	1.4	7.9	5.7	5.5	4.4	6.4	10.2	6.1
Eu	1.1	1.2	1.0	1.3	0.5	0.6	0.8	0.4	0.6	0.2	1.0	0.6	0.7	1.6	1.3	1.6	0.6	1.9
Gd	2.1	4.1	2.6	4.1	3.7	5.0	3.0	8.8	5.8	6.3	1.2	6.5	5.1	5.1	4.3	5.6	8.9	7.5
Tb	0.3	0.6	0.5	0.6	0.6	0.8	0.4	1.4	0.9	1.0	0.2	1.0	0.8	0.8	0.7	0.8	1.6	1.1
Dy	1.9	3.7	3.1	4.0	3.7	4.9	2.5	9.1	6.0	6.6	0.9	6.5	5.5	4.8	4.7	5.2	10.6	6.2
Ho	0.4	0.7	0.7	0.9	0.8	1.0	0.5	1.9	1.3	1.4	0.2	1.4	1.2	1.0	1.0	1.1	2.3	1.2
Er	1.1	1.8	1.3	2.4	2.4	3.0	1.4	5.6	3.7	3.8	0.6	4.1	3.4	2.7	2.8	3.0	6.3	3.6
Tm	0.2	0.3	0.2	0.4	0.4	0.5	0.2	0.9	0.6	0.6	0.1	0.6	0.6	0.4	0.4	0.4	1.0	0.5
Yb	1.0	1.7	1.3	2.4	2.9	3.1	1.5	6.1	4.1	4.1	0.8	4.4	3.9	2.5	2.7	3.0	6.8	3.2
Lu	0.2	0.3	0.2	0.4	0.5	0.5	0.2	1.0	0.7	0.6	0.1	0.7	0.6	0.4	0.4	0.5	1.1	0.5
Hf	0.9	3.0	1.6	3.5	4.6	6.4	3.3	13.2	8.2	4.7	4.2	9.2	9.4	4.0	3.9	7.7	5.9	1.2
Ta	0.2	0.5	0.3	0.6	1.5	1.2	1.1	3.0	1.2	1.6	0.5	1.6	0.9	0.8	0.4	0.8	3.0	0.4
Th	0.9	1.7	1.0	4.9	16.9	15.2	14.0	20.8	16.3	16.3	12.8	15.9	9.0	3.2	2.9	7.7	12.1	2.0

Columns: gd: gabbro-diorite, g: granite, a: alkali granite, f: felsic part of composite dike, hy: hybrid, e: enclave, gr: graywacke. Modal data based on 600 points. Tr: volume less than 1%, nd: not detected, n.d.: not determined. **: alteration minerals.

atomic emission spectrometry (DCP–AES) at Bryn Mawr College using the methods of Feigenson & Carr (1985). Trace-element concentrations were determined by inductively coupled plasma – mass spectrometry (ICP–MS) at Union College, Schenectady, N.Y. Replicate analyses of USGS standard samples indicate a precision of ±2% for major elements and ±5% for trace elements.

Rock powders were prepared for determination of the $^{87}Sr/^{86}Sr$ isotopic ratio by standard acid wash and Sr elution techniques. Each unspiked whole-rock sample was dissolved in an HF–HNO_3 mixture using Savillex dissolution bombs at ~100°C for seven days. The entire solution was centrifuged and processed to separate Sr using ion-exchange techniques. $^{87}Sr/^{86}Sr$ values were determined on an automated VG–54 mass spectrometer at Virginia Polytechnic Institute and State University, Blacksburg, Virginia. The values were corrected for fractionation using $^{87}Sr/^{88}Sr$ equal to 0.1194. York's (1969) approach in the least-squares regression treatment of data assumed an experimental error of 1% in $^{87}Rb/^{86}Sr$ and 0.05% in $^{87}Sr/^{86}Sr$.

Five fission-track (FT) ages and FT length-distribution patterns were obtained for selected rocks. Apatite fractions were separated using conventional heavy-liquid and magnetic techniques. Sample preparation and analyses were conducted at the University of Pennsylvania, Philadelphia, Pennsylvania. Samples were irradiated at the U.S. Geological Survey facility, Denver, Colorado. Apatite FT ages were measured using the external detector method (Naeser 1976). Preparation procedures, neutron-dose calibration, and track-length measurements on apatite mounts were carried out using the methods of Omar *et al.* (1987). Uncertainties of ages were determined by calculations described by Green (1981).

Geochronology

The distribution of radiogenic ages in the Burnett Inlet Igneous Complex is shown on Figure 2. The K/Ar hornblende and biotite dates are from granitic rocks reported by Douglass *et al.* (1989). Our Sr isotope and apatite FT data add to the geochronological history of the area. Table 2 lists the whole-rock Sr and Rb isotopic abundances for selected gabbro and granite samples. The $^{87}Rb/^{86}Sr$ values were calculated using measured amounts of elemental Rb and Sr. The initial $^{87}Sr/^{86}Sr$ ratio (SIR) was calculated using an age of 20 Ma from the K/Ar hornblende and biotite ages of Douglass *et al.* (1989). The calculated SIR of the mafic rocks ranges from 0.70411 to 0.70482 (±0.00035). The felsic rocks show a range of Rb–Sr isotopic abundances; they form an isochron with a slope of 3.192×10^{-4} and *y* intercept (SIR) of 0.70465 ± 0.00028 (Fig. 4). Calculation of a crystallization age from the slope of the isochron yields t = 22.47 ± 2.1 m.y.

Combined apatite FT ages and horizontal confined track-length distribution patterns are presented in Figure 5. Apatite FT ages range from 17.3 ± 2.3 to 25.6 ± 5.8 Ma. All length distributions are unimodal and fairly narrow, with mean track-lengths ranging from 11.92 ± 1.9 to 14.64 ± 1.14 μm. The average track-length for the fourteen analyzed samples is 13.73 ± 0.95 μm. Note

TABLE 2. Rb-Sr ISOTOPOIC DATA FOR SELECTED BURNETT INLET IGNEOUS COMPLEX ROCKS, SOUTHEASTERN ALASKA

Sample	Rock Type	Rb[a]	Sr[a]	Rb/Sr	$^{87}Rb/^{86}Sr$ calculated	$^{87}Sr/^{86}Sr$[b] measured	$^{87}Sr/^{86}Sr_{init}$[c] calculated
9219	gd	13	599	0.02	0.0627	0.70484	0.70482
9222	gd	25	431	0.06	0.1677	0.70465	0.70460
92341	gd	41	447	0.09	0.2652	0.70466	0.70459
9236	gd	22	619	0.04	0.1028	0.70414	0.70411
92492	gd	33	586	0.06	0.1628	0.70478	0.70473
9216	g	149	116	1.28	3.7136	0.70610	0.70505*
9230	a	149	79	1.89	5.4529	0.70647	0.70492*
9244	a	143	45	3.18	9.1874	0.70726	0.70465*
9248	a	170	32	5.31	15.3592	0.70985	0.70549*
927H	f	131	35	3.74	10.8211	0.70785	0.70478*
9231H	f	68	370	0.18	0.5313	0.70497	0.70482*
92503H	f	76	174	0.43	1.2628	0.70485	0.70449*

Rock abbreviations as in Table 1.

[a] Rb and Sr concentrations by ICP-MS analyses.

[b] Measured $^{87}Sr/^{86}Sr$ given at 95% confidence level.

[c] Initial $^{87}Sr/^{86}Sr$ isotopic ratio calculated from 20 Ma age based on K-Ar determination on hornblende and biotite from the same locality reported by Douglass *et al.* (1989).

* Initial $^{87}Sr/^{86}Sr$ isotopic ratio from whole rock isochron = 0.70465.

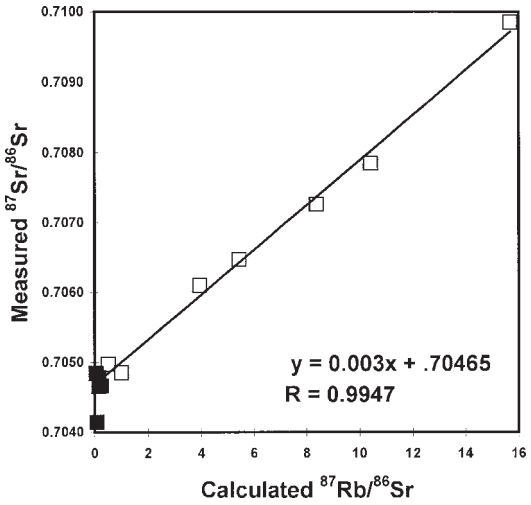

FIG. 4. Whole-rock Rb–Sr isotope data for selected gabbroic (solid squares) and granitic (open squares) rocks from the Burnett Inlet Igneous Complex. Data for the granitic rocks form an isochron indicating a crystallization age of 22.47 million years and a *y*-intercept (SIR) of 0.7047.

that all radiogenic ages (apatite FT, whole-rock Rb/Sr, hornblende and biotite K/Ar) are concordant within analytical uncertainty (Fig. 5F). The concordance of ages, despite the fact that the radiometric systems examined have markedly different closure temperatures, is consistent with very rapid cooling. Rapid cooling also is suggested by the narrow apatite track-length patterns (standard deviation 1.47, median length 13.85 μm, average 13.53 μm). The concave-up temperature *versus* time curve indicates that the cooling history of the pluton was dominated by the rapid decay of any initial difference in temperature between pluton and host rocks (Harrison *et al.* 1979, Harrison & Clarke 1979, Zeitler 1985).

PETROGRAPHY

Granitic rocks

Granitic rocks occur as outcrops of massive, uniform granite and alkali feldspar granite, as well as the leucocratic matrix surrounding enclaves in composite zones. The granite unit consists primarily of granite but includes granodiorite, quartz monzonite and quartz syenite. On average, the granite contains major alkali feldspar (36%), quartz, (32%), plagioclase (26%), hornblende (5%), and biotite (1%), with accessory ilmenite, magnetite, apatite, zircon, and titanite (numbers in parentheses are averages of seven modal analyses). Most samples have an anhedral granular to seriate texture. Graphic and granophyric intergrowths are common. Subhedral to rare euhedral plagioclase tablets display normal zoning ($An_{32–16}$) and simple and polysynthetic twinning, and may be enclosed by alkali feldspar. These features suggest that plagioclase preceded alkali feldspar in the crystallization sequence, and that alkali feldspar precipitation outlasted that of plagioclase. Hornblende is commonly euhedral and occurs intergrown with plagioclase, alkali feldspar and quartz, whereas biotite is an anhedral interstitial phase. Both hornblende and biotite exhibit minor and partial alteration to chlorite. Ilmenite, magnetite, apatite, zircon and titanite form euhedral phases.

The alkali feldspar granite occurs as a massive homogeneous unit to the west of the granite on Etolin Island (Fig. 2). It consists primarily of interlocking subhedral perthitic alkali feldspar (54%) and anhedral quartz (37%), with interstitial plagioclase (2%), hornblende (3%), biotite (1%) and opaque phases (3%) (numbers in parentheses are averages of seven modal analyses). Accessory euhedral apatite, titanite, and zircon are common within the unit. Brew *et al.* (1984) reported an unusual mafic mineral assemblage in the alkali granite unit: sodic hornblende, riebeckite, biotite, Fe-rich pyroxene and fayalite. Our examinations of eight alkali feldspar granites found only one sample (9256) containing fayalite and pyroxene; we did not observe sodic hornblende nor riebeckite.

The leucocratic matrix phase surrounding mafic magmatic enclaves in the composite zones exhibits a range of compositions including monzodiorite, granodiorite, granite, quartz monzonite, and monzonite. Subhedral interstitial hornblende and biotite are more abundant in the leucocratic enclave matrix than in the granite and alkali feldspar granite plutons.

On the basis of grain form and relationships, the following sequence of crystallization is proposed for the granitic rocks: early plagioclase, hornblende, ilmenite, magnetite, apatite, zircon and titanite; continued plagioclase crystallization with alkali feldspar, quartz and biotite; latest alkali feldspar, quartz and biotite.

Mafic rocks

The medium- to coarse-grained gabbro–diorite consists primarily of tablets (1 by 3 mm) of albite-twinned normally zoned ($An_{63–58}$) euhedral plagioclase, anhedral clinopyroxene, orthopyroxene, hornblende and biotite. Plagioclase and clinopyroxene commonly exhibit a subophitic texture. A few samples contain abundant and crowded cumulate calcic plagioclase tablets with minor mafic intergranular and interstitial phases. Rare olivine forms anhedral equant crystals. Reddish brown pleochroic hornblende is ubiquitous and occurs as a mantle on olivine, clinopyroxene and orthopyroxene, as anhedral oikocrysts, and as prismatic crystals. Magnetite and ilmenite occur as euhedral to subhedral primary phases as well as products of decomposition of olivine and orthopyroxene. Euhedral apatite forms inclusions in the

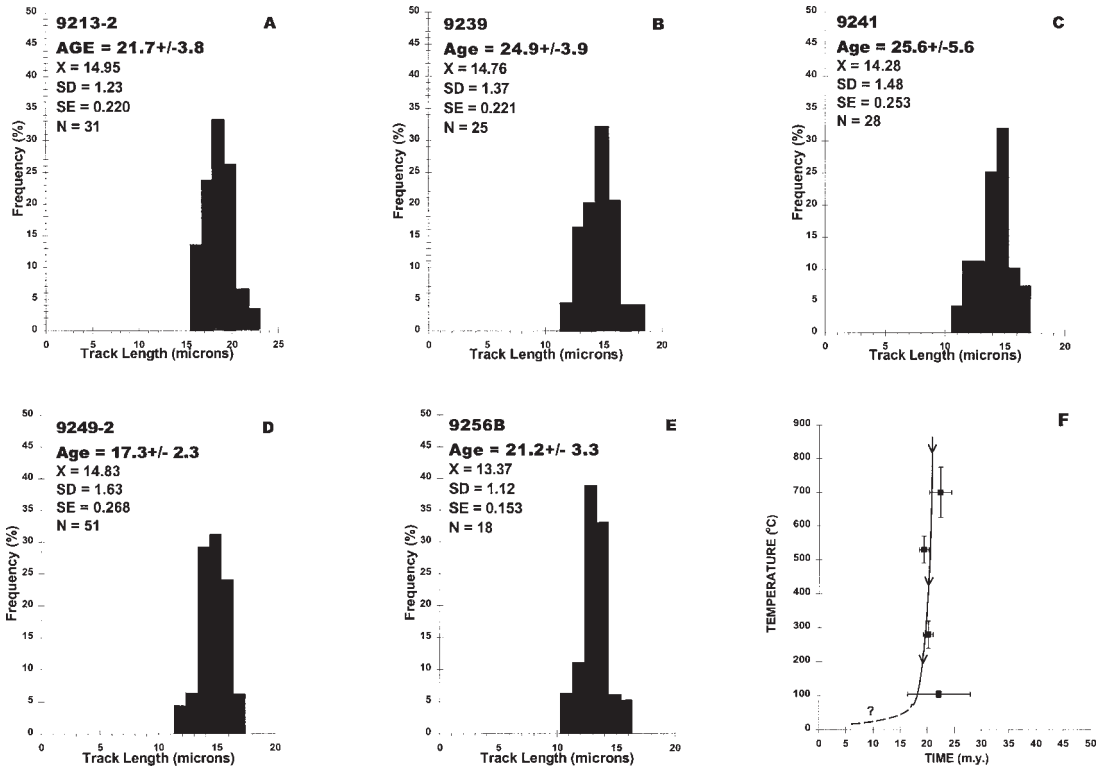

FIG. 5. A through E. Frequency distribution of the lengths of confined spontaneous fission tracks in apatite. Ages and frequency-distribution data are shown in upper left-hand corner of histograms. AGE: fission track age determined by external detector method, X: mean fission-track length, SD: standard deviation, SE: standard error for average, N: number of grains. F. Apparent cooling history for the Burnett Inlet Igneous Complex. Closure temperature – age curve is best fit to available data. Uncertainties in ages and closure temperatures are shown by error bars through symbols. Sources of age data: K/Ar ages: Douglass *et al.* (1989); Rb/Sr whole-rock age: this study; apatite FT ages: this study. Closure temperatures: biotite K/Ar: 280°C ± 40; hornblende K/Ar: 530°C ± 40; whole-rock Rb/Sr: 700°C ± 75; apatite fission-track: 105°C ± 10 (Gleadow & Brooks 1979, Harrison *et al.* 1979, Harrison & McDougall 1980). Closure temperature values are considered broadly applicable to relatively high rates of cooling.

primary mafic phases and discrete grains. Alteration products include fibrous amphibole, chlorite, talc and white mica. The gabbro–diorite unit also includes monzodiorite and quartz monzodiorite. These rocks lack olivine and orthopyroxene, but they contain clinopyroxene as discrete grains and as cores surrounded by hornblende. They consist primarily of subhedral granular plagioclase ($An_{47.7–25.5}$), hornblende, biotite, alkali feldspar and interstitial quartz.

In the composite zones, mafic enclaves display random, uniform, igneous microtextures. Two types dominate: very fine-grained plagioclase – biotite – hornblende assemblages with an anhedral granular texture, and porphyritic rocks containing plagioclase ± clinopyroxene phenocrysts. Other major phases include orthopyroxene, quartz, and alkali feldspar. Ilmenite and apatite are common accessory phases. Phenocrysts of olivine were noted in only a few enclaves, and in some cases olivine had recrystallized to an aggregate of very fine-grained talc and lizardite. In the porphyritic samples, plagioclase occurs as euhedral to swallow-tail single crystals and as glomerocrysts (Fig. 6A). Clinopyroxene phenocrysts are subhedral and commonly mantled by green pleochroic hornblende. In the anhedral granular enclaves, brown pleochroic hornblende and orange-brown pleochroic biotite are commonly poikilitic and in some cases acicular in form. Apatite always occurs as acicular grains. A few enclaves contain 1–2 mm anhedral quartz crystals mantled by green hornblende (Fig. 6B). Enclave matrices contain spotty concentrations of dendritic opaque minerals (Fig. 6C).

The mineralogy of the hybrid rocks includes plagioclase, hornblende, biotite, alkali feldspar, quartz ± clinopyroxene ± orthopyroxene and accessory ilmenite

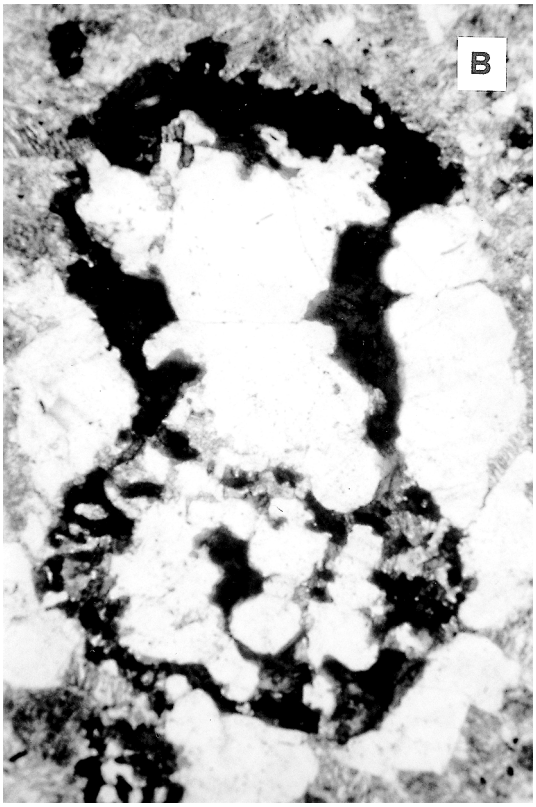

and apatite. Some of the textures are similar to those noted in the enclaves, such as plagioclase and clinopyroxene phenocrysts, hornblende mantles on clinopyroxene phenocrysts (Fig. 6D), poikilitic hornblende and biotite, and acicular apatite. Micro-inclusions in these rocks consist of centimetric round aggregates of fine-grained anhedral biotite, hornblende, plagioclase and quartz.

Textural relationships indicate that the mafic plutons, mafic enclaves, and hybrid rocks share a similar sequence of crystallization: early-crystallizing olivine, magnetite, ilmenite, apatite, and plagioclase, ± orthopyroxene ± clinopyroxene; continued crystallization of plagioclase and clinopyroxene, with the formation of hornblende, and latest-crystallizing hornblende, biotite, quartz and alkali feldspar. The variable grain-sizes and textures of members of the mafic suite are the results of different histories of crystallization. The coarse to medium size and common subophitic texture of the gabbro–diorite suggest slow *in situ* cooling and crystallization. The weak outcrop-scale layering with cumulate plagioclase zones suggests some plagioclase accumulation, although the extent of accumulation is unknown.

The porphyritic enclaves experienced a two-stage history of crystallization. Initial slow crystallization produced euhedral plagioclase and clinopyroxene phenocrysts following by rapid nucleation and formation of the fine-grained matrix. The fine-grained rock textures resulted from a rapid drop in magma temperature, as further demonstrated by the quench textures of dendritic ilmenite and acicular apatite (Lofgren 1980, Wyllie *et al.* 1962). On the basis of the occurrence of the fine-grained mafic rocks, we infer that rapid cooling and crystallization of enclave and hybrid magmas occurred when mafic magma came into contact with much cooler granitic magma (a temperature difference of 200–400°C).

A number of the textures observed in the hybrid rocks and in some enclaves are common to and characteristic of mixed magma–hybrid systems (Hibbard 1995). In the context of magma mixing, crystallization of abundant quench-generated plagioclase and apatite was followed by late-stage poikilitic hornblende and biotite. The relatively large rounded quartz grains with a thin rim rich in fine-grained earlier-crystallizing mafic minerals are interpreted as xenocrysts from the crystallizing granitic liquid. As the magmas mixed, quartz crystals from the felsic component liquid became un-

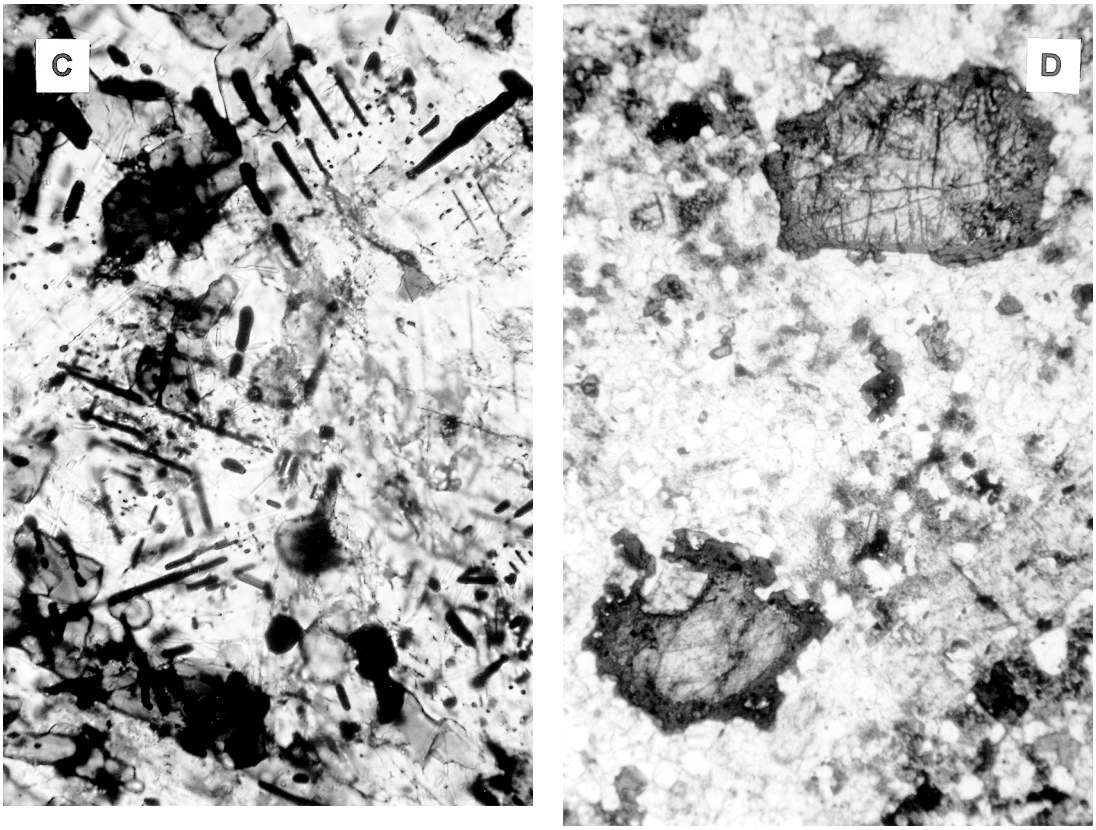

FIG. 6. A. Photomicrograph of plagioclase-phyric enclave (92524e). Plagioclase phenocryst exhibits swallow-tail form (plane-polarized light, long dimension: 1.07 mm). B. Photomicrograph of enclave (9256) containing a quartz xenocryst mantled by green hornblende in a very fine-grained anhedral granular matrix (plane-polarized light, long dimension: 3 mm). C. Photomicrograph of very fine-grained anhedral granular enclave (92503e) containing dendritic acicular grains of ilmenite (plane-polarized light, long dimension: 1.07 mm.). D. Photomicrograph of hybrid rock (92351) containing clinopyroxene phenocrysts in an anhedral granular matrix of plagioclase, quartz, alkali feldspar and biotite. Clinopyroxene is mantled by green hornblende (cross-polarized light, long dimension: 3 mm).

stable (Hibbard 1981, Vernon 1983, 1984, 1990). The quartz grains, now xenocrysts in the hybrid magma, were partially dissolved and served as substrates for the nucleation of precipitating mafic minerals. Mafic micro-inclusions probably represent droplets of mafic magma that were incorporated into and dispersed throughout the relatively more silicic magma. The hornblende mantles on anhedral clinopyroxene observed in both enclave and hybrid rocks could have resulted from the discontinuous reaction of clinopyroxene to hornblende during the slow cooling stage of enclave crystallization (Vernon 1983), facilitated by the addition of H_2O during magma mixing.

GEOCHEMISTRY AND PETROGENESIS

Representative bulk compositions are presented in Table 1 and Figure 7. Complete results are available upon request. The granite suite rocks show many of the compositional attributes of A-type, anorogenic granites (*e.g.*, White & Chappell 1983, Whalen *et al.* 1987). They are subalkaline and metaluminous to marginally peraluminous, with enrichment of incompatible elements (K, Zr, Nb) and depletion of compatible elements (Cr, Ni, Ba, Sr) relative to other granite types with comparable silica contents. The rocks of the granite suite also correspond to the I-type classification of Chappell

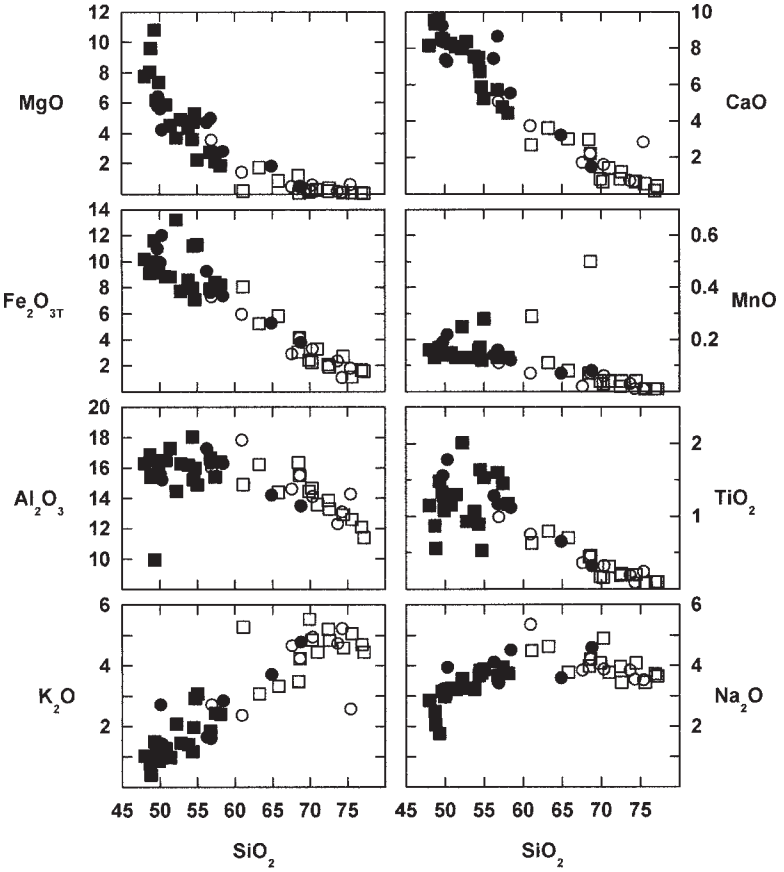

& White (1974). They have relatively high sodium (>3.2 wt.% Na_2O), < 1% normative corundum, SIR between 0.704 and 0.706, an absence of modal aluminous minerals, and contain mafic magmatic inclusions. The mafic rocks are subalkaline and show a moderate Fe-enrichment from low-silica to high-silica members.

Compositions of Burnett Inlet Igneous Complex rocks vary widely between 48 and 78 wt.% SiO_2 and 11 to 0.12 wt.% MgO. Although there are a few intermediate-composition samples that bridge the gap between the relatively mafic (48–60 wt.% SiO_2) and relatively felsic (65–78 wt.% SiO_2) suites, many elemental trends are continuous between the two groups. As SiO_2 increases, levels of MgO, CaO, Fe_2O_{3T} and Sr decrease. Concentrations of Cr, Ni, and Co decrease regularly within the mafic suite. Concentrations of Na_2O, Ba, and Zr increase with increasing SiO_2 content in the mafic rocks and decrease in the felsic rocks. The proportion of Al_2O_3 and TiO_2 are relatively constant or are somewhat scattered for the mafic rocks and decrease in the felsic rocks with increasing SiO_2. The concentration of large-ion lithophile elements K and Rb increases regularly with increasing SiO_2.

Chondrite-normalized rare-earth-element (*REE*) patterns for the felsic and mafic rocks have common features (Fig. 8). All are enriched in the light *REE* and have flat middle to heavy *REE* patterns. For the mafic rocks, *REE* patterns from Sm to Gd are generally flat, but with three exceptions: two gabbro samples (87145 and 92341) have a positive Eu anomaly, and enclave sample 9244e has a large negative Eu anomaly. Granitic samples display a negative Eu anomaly that generally increases with increasing silica.

Magma generation: felsic rocks

The miarolitic cavities, graphic intergrowths, and post-crystallization alteration indicate that the granitic rocks crystallized from an hydrous felsic magma. Late-crystallizing biotite indicates that the granite magma initially had 2.5 to 5.0% H_2O (Maaløe & Wyllie 1975, Naney 1983). Assuming that the low-silica members (≤70 wt.% SiO_2) represent undifferentiated liquids, their high concentrations of K and Ba (>5 wt.% K_2O and 1000 ppm Ba, respectively) suggest the involvement of biotite or alkali feldspar (or both) during partial melting

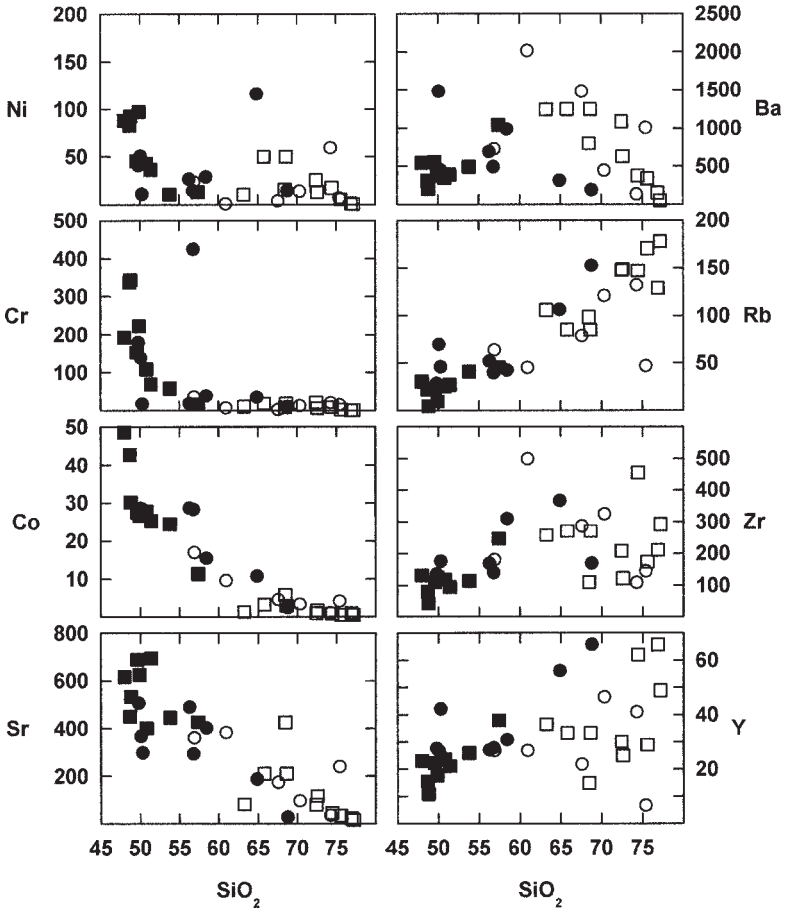

FIG. 7. Element-variation diagrams for Burnett Inlet Igneous Complex rocks. On facing page, weight % major-element oxides *versus* weight % SiO_2. Above, concentrations of trace elements (ppm) *versus* weight % SiO_2. Solid squares: gabbro–diorite, solid circles: enclaves, open squares, granite and alkali granite, open circles: felsic phase in composite zones.

of the crust. These rocks are also characterized by a small negative Eu anomaly and moderate concentrations of Sr, which suggests residual plagioclase in the source. The Sr isotopic data (granite SIR = 0.7046) imply that the source is relatively young or moderately radiogenic.

The Gravina belt that hosts the complex is composed largely of continental-margin arc-derived metagraywacke that contains a significant proportion of volcanogenic material. The juvenile and nonradiogenic composition of rocks of the Gravina terrane makes them a likely candidate to yield calcic peraluminous low-SRI silicic melts. Fluid-absent melting experiments on rocks of intermediate composition [metagraywacke: Vielzeuf & Montel (1994), tonalite: Rutter & Wyllie (1988), tonalitic gneiss: Skjerlie & Johnston (1992)] generated granitic melts through dehydration melting of biotite or amphibole (or both) leaving a weakly peraluminous granulite mineral assemblage (biotite + amphibole + quartz = orthopyroxene ± garnet + Fe–Ti oxide + granitic melt). Melting temperatures ranged from 900 to 1000°C, depending on the fluorine content of biotite. The temperatures necessary for melting could be achieved through extensive underplating of crust by basaltic magma (Wyllie 1977, 1984). In dry melting experiments (Rutter & Wyllie 1988), alkali feldspar, biotite, quartz and hornblende were progressively consumed so that only plagioclase, pyroxene and a trace of magnetite remained.

The quantitative equilibrium batch-melting equation of Shaw (1970) was applied to test whether or not it is possible to generate the *REE* concentrations in granodiorite 9239 from an unmetamorphosed and relatively

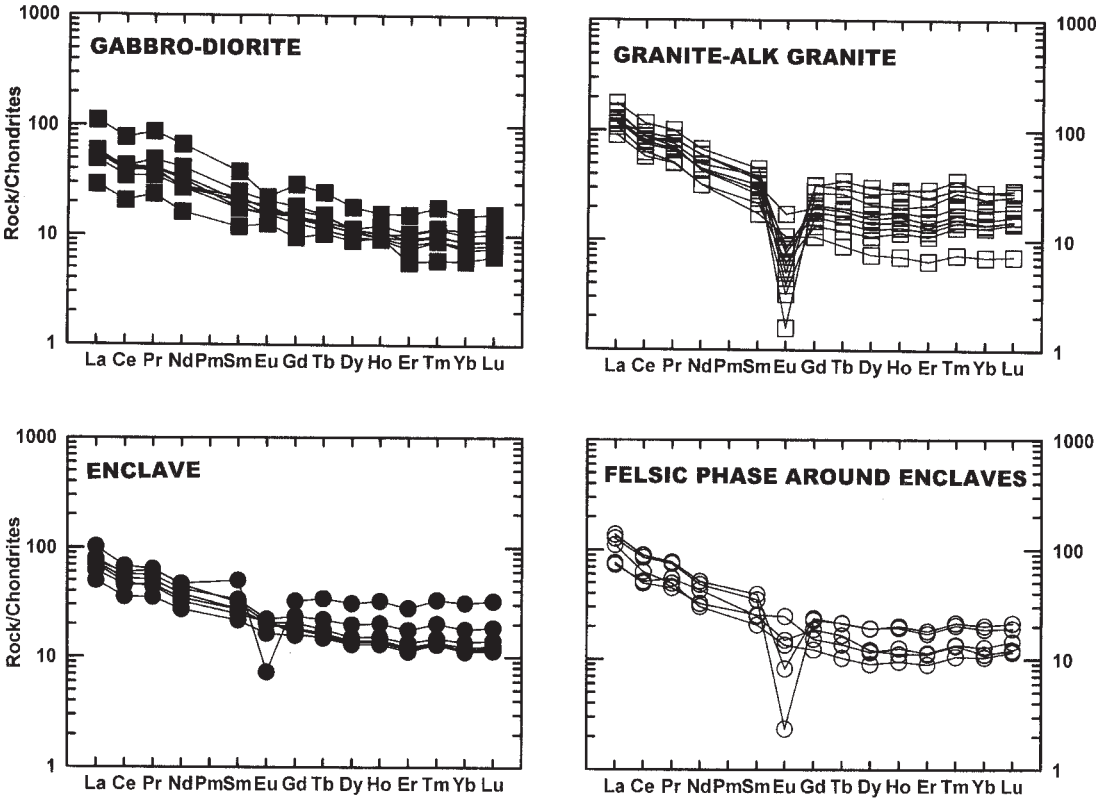

FIG. 8. Chondrite-normalized rare-earth-element diagrams for Burnett Inlet Igneous Complex rocks. Chondrite-normalization values from Nakamura (1974).

unaltered Gravina belt graywacke sample (9271). Sample 9239 was chosen to represent the undifferentiated granitic magma because of its relatively low silica content and lack of cumulate texture and alteration assemblages. Figure 9A compares the model melt composition with the composition of sample 9239. The results indicate that it is possible to generate the peraluminous granite of the Burnett Inlet Igneous Complex through 10–30% partial melting of Gravina belt crust, leaving a pyroxene- and plagioclase-rich residue.

Magma generation: mafic rocks

The mafic rocks all have similar *REE* patterns, suggesting that despite the different modes of emplacement, they evolved from similar sources. The most primitive mafic member of the suite, based on high proportion of MgO and transition-metal contents, is a two-pyroxene olivine gabbro (87145, 9219). The source of the mafic magma was modeled on the assumption that the *LREE* enrichment of the sampled mafic rocks is characteristic of a liquid in equilibrium with the source rock. The preferred and simplest model involves derivation by 5 to 10% partial melting of enriched mantle, leaving a residue of olivine + clinopyroxene + orthopyroxene (Fig. 9B).

Interactions between mafic and felsic magma

The field and petrographic data demonstrate that the mafic and felsic rocks interacted extensively to produce the composite and hybrid zones of the gabbro–diorite suite. In the composite zones, the fine-grained margins, crenulate rims, round and pillow-like shapes and igneous textures of the enclaves clearly are evidence for an origin as droplets of mafic magma emplaced within a partially or mostly liquid granitic magma. The evidence for mingling between coeval magmas rules out a direct parent–daughter relationship between the mafic component and the granite. For the same reason, the enclaves cannot represent an earlier-formed sidewall crystallized cumulate phase, subsequently incorporated into the granite. Given that the complex evolved from at least two magmas (a mafic magma and a felsic magma), we

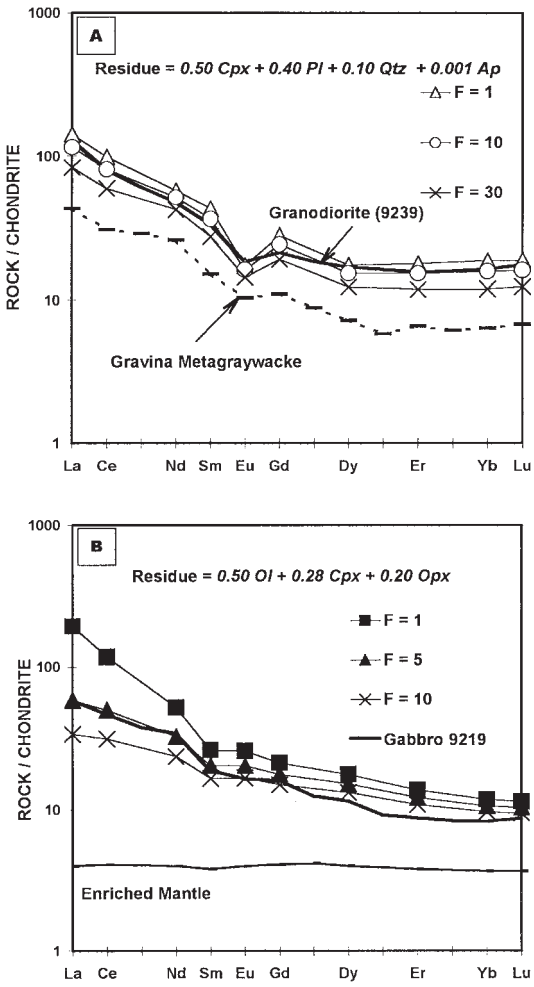

FIG. 9. Model *REE* source solutions for primitive members of the (A) felsic suite and (B) mafic suite. F: percent partial melting. Observed, model and source compositions are designated. Enriched mantle values assigned on the basis of protracted history of oceanic crust subduction in southeastern Alaska and the theoretical considerations of Pearce (1983).

now examine the geochemistry of the mafic and felsic rocks and assess the relative roles of fractional crystallization and magma mixing in influencing the overall geochemical variation.

Fractional crystallization of the felsic rocks

The granitic and alkali feldspar granitic rocks and the leucocratic matrix of composite zones are very similar to each other petrographically and chemically. Similar groupings on variation diagrams and similar *REE* patterns suggest that the various granitic rocks appear to be the products of similar batches of magma. The inverse variation of MgO, Fe_2O_{3T}, CaO, Al_2O_3 and TiO_2 with silica suggests that the primary minerals observed in thin section (plagioclase, biotite, hornblende, magnetite and ilmenite) accumulated or fractionated to produce the observed chemical variation. Several samples show high values in highly compatible elements (Ba, Sr, Zr), and presumably record crystal accumulation. The large albeit scattered decrease in Sr and Ba concentrations with silica may be attributed to fractionation of plagioclase (Sr) and alkali feldspar (Sr and Ba). The increase in the size of the negative Eu anomaly with increasing silica also is consistent with fractionation of plagioclase.

The felsic suite rocks show wide variation in several compatible elements (Ba, Sr, Eu). We modeled trace and *REE* variations within the felsic suite using simple Rayleigh fractional crystallization models. Again, we used 9239 to represent the undifferentiated parental magma. Trends displayed by Ba and La on diagrams showing these compatible elements *versus* incompatible elements (Rb and Ce) are compared to theoretical trends for fractional crystallization. Figures 10A and B show the calculated direction and magnitude of the change of magma composition (arrows) that would result from removal of the major phases determined by petrographic considerations above. Trends displayed by Ba and Rb are approximately parallel to trends predicted by removing an assemblage having the bulk distribution-coefficient corresponding to 50% plagioclase, 10% hornblende, 10% alkali feldspar, 4% magnetite, and 2% ilmenite. *REE* variations among the felsic rocks are also consistent with differentiation dominated by fractional crystallization of these rock-forming minerals. Figure 10C highlights the calculated effect of plagioclase fractionation on *REE* abundances and demonstrates the agreement between the modeled compositions and the observed *REE* compositions.

Fractional crystallization of the mafic rocks

Petrographic evidence described earlier suggests that members of the mafic suite evolved through fractionation involving olivine, orthopyroxene, clinopyroxene and plagioclase. The linear inverse variation of MgO, Fe_2O_{3T}, CaO and trace elements Ni, Cr, and Co with silica is consistent with fractionation of these major phases. We examined the variations of Ni and Cr specifically by taking the abundances of these elements found in the most primitive rock sample (9219) as starting material, and removing an assemblage having a bulk distribution-coefficient corresponding to 20% clinopyroxene, 10% olivine, 10% orthopyroxene, and accessory ilmenite. The trends displayed by Ni and Cr in Figures 11A and B are in agreement with the calculated direction and magnitude of the change in liquid compo-

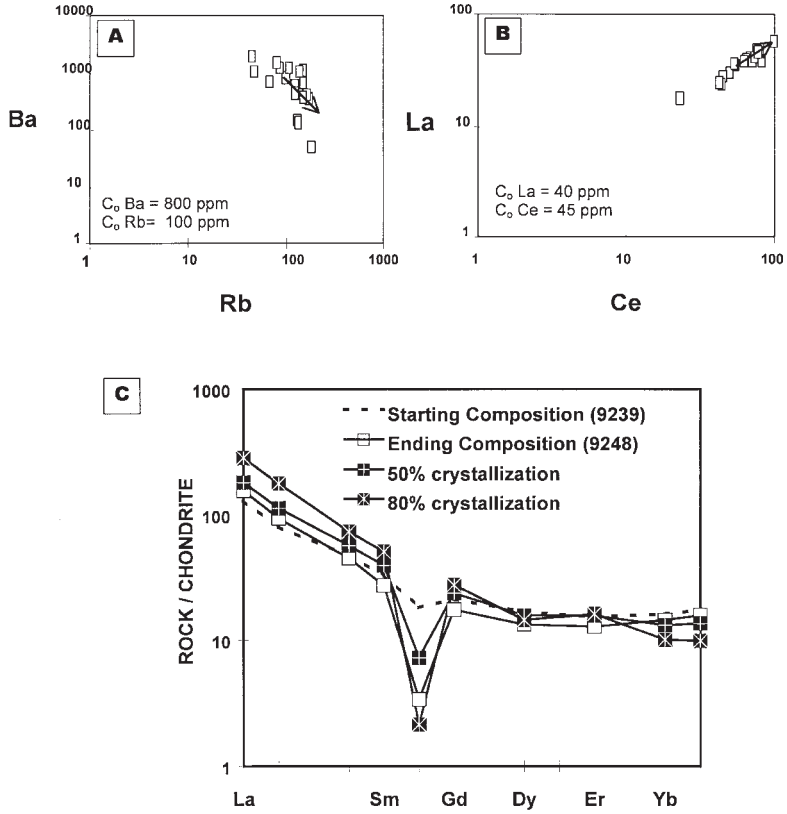

FIG. 10. Model solutions for fractional crystallization of the felsic suite. A– B. Trace-element variation diagrams, with arrows showing the direction and magnitude of Ba and La variation that would result from subtraction of the assemblage 0.50 Pl + 0.10 Hbl + 0.10 Or + 0.04 Mgt + 0.02 Ilm from a granodioritic liquid (9239) with the indicated initial compositions (C_o). C. Chondrite-normalized *REE* variations resulting from fractional crystallization of the same assemblage used in A. Mineral/liquid distribution coefficients used in calculation are those for rhyolite, taken from the compilation of Rollinson (1993).

sition that would arise from removing the mafic minerals noted. Likewise, *REE* abundances are consistent with differentiation dominated by fractional crystallization of these rock-forming phases plus plagioclase. The development of a slight negative Eu anomaly in samples of differentiated gabbro and enclaves suggests minor fractionation of plagioclase (Fig. 11C). The positive Eu anomaly in cumulate gabbro reflects the accumulation of plagioclase.

Magma mixing

Whereas we have demonstrated above that fractional crystallization and accumulation were important processes affecting the geochemical evolution of the complex, the Sr isotopic data suggest the involvement of mixing of felsic and mafic magmas. Crawford *et al.* (1995) studied a suite of Recent volcanic rocks that intruded several lithostratigraphic units in the area (the Alexander terrane, Gravina terrane, and the Coast Plutonic Complex). They used Sr isotopic data to demonstrate that the mantle underlying southeastern Alaska during the Neogene was homogeneous and had an initial $^{87}Sr/^{86}Sr$ ratio of 0.7023. Considering this, the 0.7046 value for the 20 Ma gabbro is relatively high and suggests contamination from the comagmatic granite. The association of crust-derived granite and mantle-derived gabbro at the present level of exposure, as well as the commingled relationship between enclave and granitic rocks, make it highly likely that mafic and felsic liquids interacted during their ascent. Although the addition of mafic material into the granitic magma would

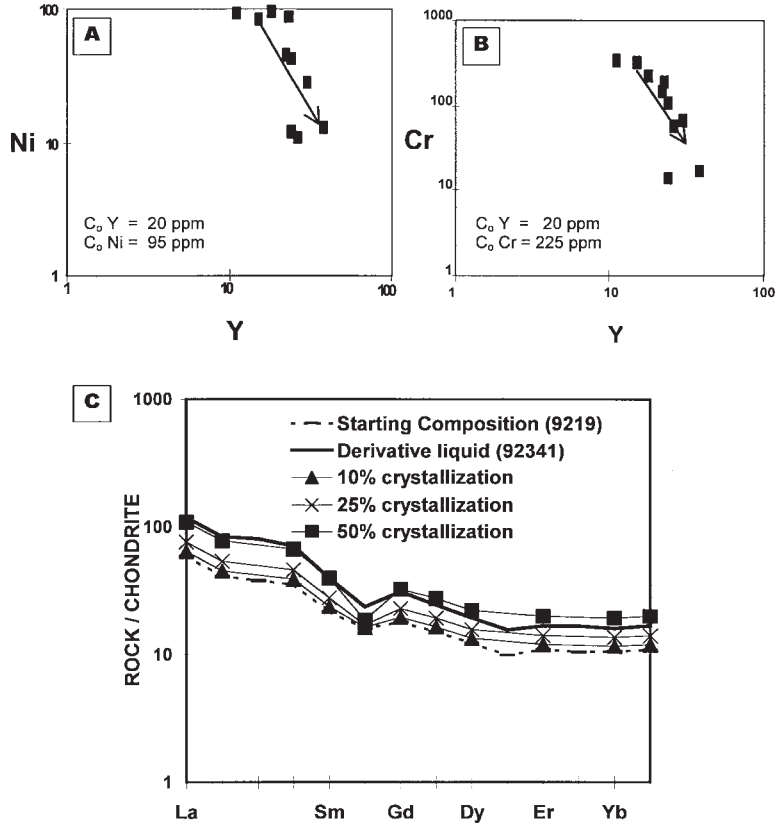

FIG. 11. Model solutions for fractional crystallization of the mafic suite. A–B. Trace-element variation diagrams, with arrows showing the direction and magnitude of Ni and Cr variation that would result from subtraction of the assemblage 0.30 Cpx + 0.10 Opx + 0.10 Ol + 0.01 Ilm from a basalt liquid (9219) with the indicated initial compositions (C_o). C. Chondrite-normalized *REE* variations resulting from fractional crystallization of the same assemblage used in A. Mineral/liquid distribution coefficients used in calculation are those for basalt, taken from the compilation of Rollinson (1993).

have little effect in lowering the SIR of the granite, the addition of felsic material, having a higher amount of radiogenic Rb, would have a major effect on the Sr isotopic composition of the magma responsible for the gabbro–diorite.

The textures suggest that magma mixing may have occurred locally; however, the chemical evidence does not support a bulk-mixing model between granitic and basaltic end-members. In particularly, variations of TiO_2, Na_2O, Ba, Y, and Zr with silica show distinctly different trends in the mafic and felsic rocks, suggesting that each suite evolved independently, from a separate magma.

Mixing of two magmas is controlled primarily by their bulk compositional and thermal differences (McBirney 1980, Furman & Spera 1985). Large compositional and thermal differences between the two magmas inhibit mixing, whereas smaller differences permit hybridization. Rheologic modeling by Frost & Mahood (1987) indicates that homogenization of two magmas is unlikely if the compositional difference between them exceeds 10 wt.% SiO_2. On the basis of these considerations, the observed compositional contrast in most enclave–host pairs is too large to have allowed large-scale mixing and precludes a mixing model involving end-member granitic and basaltic magmas. However, the efficacy of magma mixing would have increased if episodes of magma mixing within the complex involved intermediate composition magmas (granodiorite into basalt; diorite into granite). It is possible that basaltic magma mixed with a granodioritic magma before extensive crystallization of the felsic magma. It is also possible that an evolved mafic magma (dioritic, granodioritic) mixed with the granitic magma some time

in its history. In either of these cases, the relatively smaller compositional and thermal contrast between the participating magmas could allow magma mixing and hybridization.

Figure 12 shows the results of modeling of magma mixing for MgO and Ba. The trends modeled by mixing of end-member basaltic and granitic magmas clearly do not match the observed trends in the data on mafic and felsic rocks. There is a better fit to the observed data when mixing models include intermediate magma compositions (diorite, granodiorite). Although these latter models do not reproduce the actual trends in the mafic and felsic rocks, they better approximate the geochemical variation within the Burnett Inlet Igneous Complex.

Conditions of Pluton Emplacement

During the Eocene (about 43 Ma), changes in relative motion of plates resulted in a shift in Pacific – North America plate interactions in the southeastern Alaska – coastal British Columbia region, from oblique convergence to mainly dextral transcurrent motion (Engebretson *et al.* 1985, Stock & Molnar 1988, Lonsdale 1988, Engebretson 1989). In the overall strike-slip tectonic setting that characterized post-Eocene plate motions in the study area, either transtension or transpression may have occurred (Conway *et al.* 1995). Post-Eocene extension-related sedimentation, volcanism, and plutonism have been well documented in the Queen Charlotte Basin about 250 km south of the study area (Lewis *et al.* 1991, Rohr & Furlong 1995). Our chemical evidence supports an interpretation that the bimodal Burnett Inlet Igneous Complex originated within this extensional tectonic regime. Tectonic discriminant diagrams (Fig. 13) show that the mafic rocks have characteristics of within-plate basalt consistent with an extensional setting. On the trace-element discriminant diagram of Shervais (1982) (Fig. 13B), the mafic rocks plot in the mid-ocean

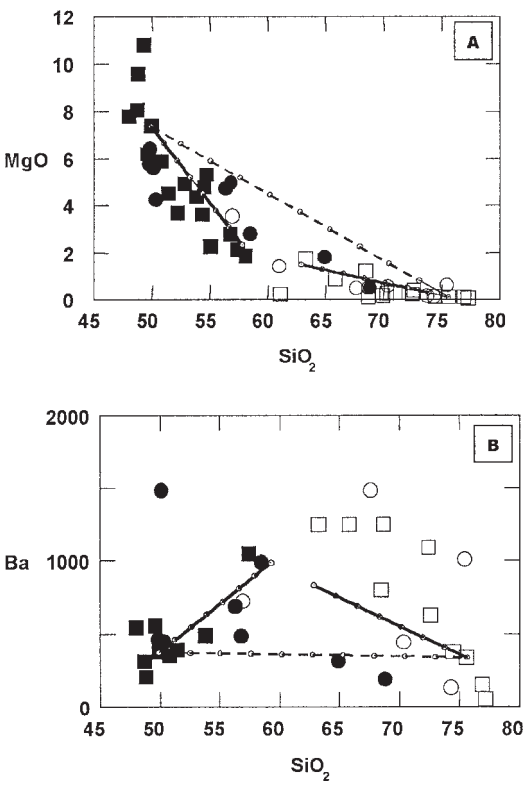

FIG. 12. Magma-mixing models. Dashed lines show the trends expected for mixing basaltic and granitic magmas. Solid lines show the trends expected for mixing magma of intermediate silica content (granodioritic) into basaltic magma on the left and an evolved basalt (diorite) into granite on the right. Symbols used are the same as in Figure 7.

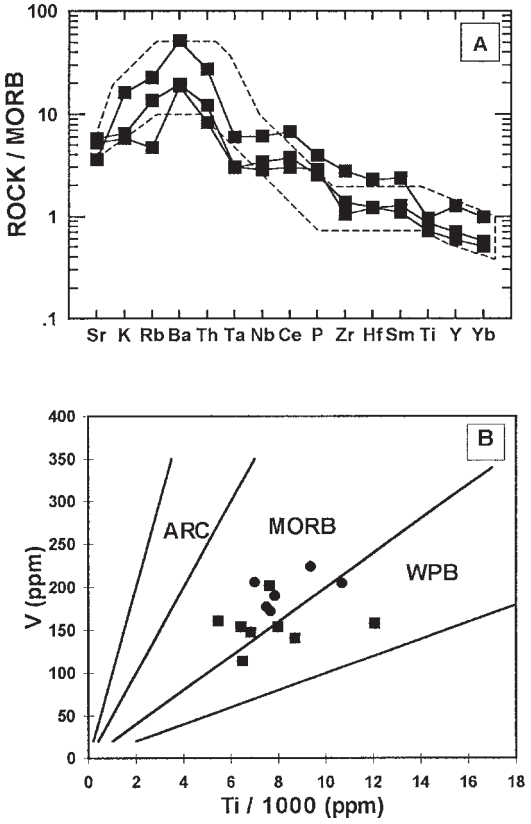

FIG. 13. A. MORB-normalized distribution of elements in selected mafic rocks. Dashed envelope shows area of known within-plate basalts from Antarctica (Kyle 1981) and Ethiopia (Brotzu *et al.* 1981). B. V–Ti discriminant diagram for mafic rocks, after Shervais 1982. Symbols used are the same as in Figure 7.

ridge basalt (MORB) and within-plate basalt (WPB) fields. The granites also show within-plate attributes (Fig. 14). All are high in Rb and Th, and moderately to largely depleted in Ba compared to ocean-ridge granite (Pearce *et al.* 1984). Except for Ba, the granites show a general decrease in the trace-element concentrations from Rb to Yb, a feature of "crust-dominated" processes (Pearce *et al.* 1984). On trace-element tectonic discriminant diagrams (Pearce *et al.* 1984), the studied granites overlap the fields of volcanic arc granite (VAG) and within-plate granite (WPG) (Fig. 14B). The position of some of the samples in the VAG field may reflect the process of plagioclase accumulation, since plagioclase is compatible with the elements used in the discriminant diagrams. Alternatively, the trace-element concentrations may have been inherited from source rocks that were generated in a volcanic arc environment. In sum, the Burnett Inlet Igneous Complex comprises magmatic rocks that originated during transtension.

Our interpretation of the generation and emplacement of the Burnett Inlet Igneous Complex is shown in Figure 15. The numbers in the discussion below are keyed to this figure. Tectonic extension resulted in decompression-induced mantle melting and generation of basalt (1). Mafic magma ponding at the base of the crust triggered partial melting and the formation of granite (2). The basaltic magma served as the heat source necessary for vapor-absent melting reactions. Some of these melts rose through the crust along extensional zones of crustal weakness (3) and were emplaced at shallow lev-

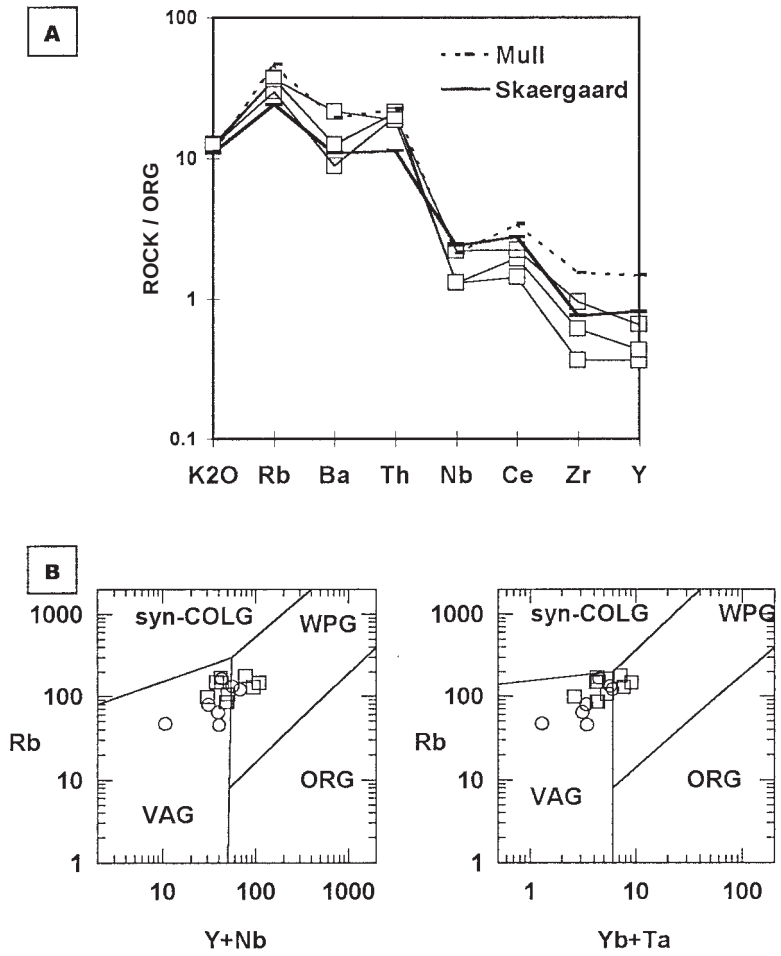

FIG. 14. A. Trace-element patterns for selected granites normalized to concentrations in average ocean-ridge granite (ORG). Patterns for granites from within-plate settings (Mull and Skaergaard) are plotted for comparison; data from Pearce *et al.* (1984). B. Tectonic discriminant diagrams for granites after Pearce *et al.* (1984).

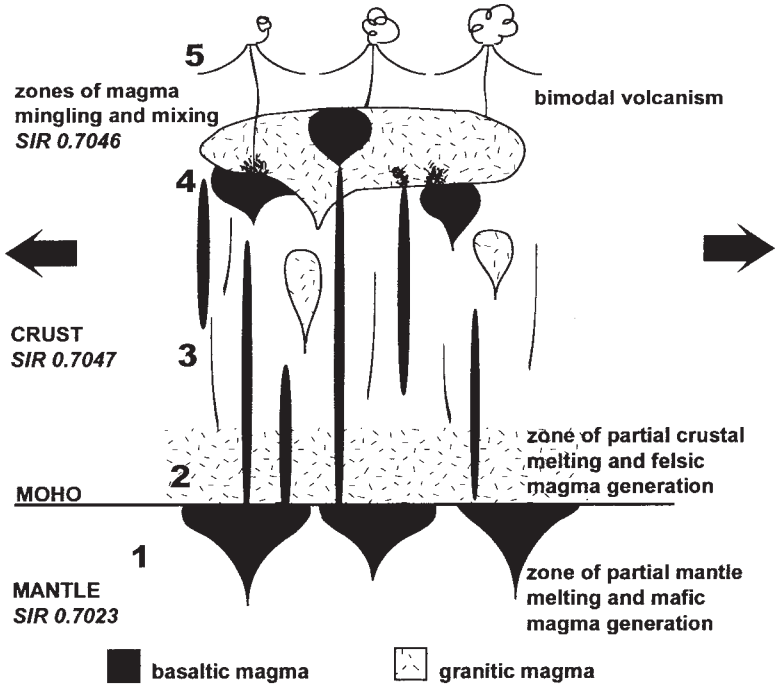

FIG. 15. Schematic illustration of the formation and emplacement of the Burnett Inlet Igneous Complex. Numbers are discussed in text.

els in the crust (4). The plutons imparted a low-pressure, high-temperature cordierite-bearing thermal aureole to the country rocks (Duggan 1987, Gerdes 1988). Geobarometers in the contact-metamorphic aureoles suggest emplacement at 0.75–1.5 kbar (Cook 1991). Assuming an average density of crust of 2800 kg/m^3, these pressure estimates correspond to an emplacement depth of 3 to 6 km. The abundant miarolitic cavities observed in the granite are consistent with a shallow level of emplacement. On the basis of an estimated paleogeothermal gradient of 20°C/km for the Coast Mountains of British Columbia ($24^{+13}/_{-8}$°C/km at 35 Ma, and $17\ ^{+8}/_{-6}$°C/km at 20 Ma; Parrish 1983) and an average surface temperature of 10°C, a depth of emplacement 3 to 6 km coincides with temperatures of 70 to 130°C. The radiogenic ages and apatite FT length-distribution profiles (Figs. 2, 5) provide additional information for a reconstruction of the geological history of the complex. The concordant results from all geochronological systems (apatite fission tracks, biotite K/Ar, hornblende K/Ar, and whole-rock Rb/Sr) lead us to favor emplacement in host rocks less than 105°C. This temperature is below the thermal stability of apatite fission tracks (105°C) and would correspond to burial depths of <4.5 km given the assumed geothermal gradient cited above. Although it is difficult to reconcile the medium to coarse texture throughout the complex with the geochronological evidence for rapid cooling, it is possible that the hydrous nature of the granitic magma facilitated the development of a coarse grain-size.

Heat-conduction models (Carslaw & Jaeger 1959, Larsen 1945) indicate that once the initial difference in temperature between pluton and host rocks decays, conductive loss of heat to the walls of the intrusion has little influence on cooling time, except in the immediate vicinity of the igneous complex. Likewise, a sedimentary cover has little effect on cooling times for any point within the intrusion, except where the cover is very thick or near the pluton contact. We suggest that the most likely cause for rapid cooling of the plutonic complex is explosive volcanism (5, Fig. 15). The mafic magmatic enclaves common throughout the complex document that mafic dikes intersected the granitic magma chamber. This scenario allows for the possibility that the basaltic intrusion that resulted in magma mixing may also have had a role in causing the explosive eruption of the magma chamber of the Burnett Inlet Igneous Complex. Sparks *et al.* (1977) proposed magma mixing as a possible mechanism for triggering eruptions of silicic volcanos. In their model, intrusion of basalt into a silicic magma chamber causes superheating and convection of the silicic magma, resulting in entrainment and physical mixing of some of the basalt. Superheating and decompression of parts of the silicic magma due to con-

vection can lead to supersaturation of volatile phases and vesiculation. Pressure exerted on the confining walls of the magma chamber is increased by addition of basalt and by vesiculation of the silicic magma. The pressure increase may be sufficient to fracture the volcanic edifice and trigger an explosive eruption. Our data for rapid cooling thus provide evidence to support the suggestion by previous authors (Brew *et al.* 1981, Hunt 1984) that some of the plutons of the Kuiu–Etolin Igneous Belt may represent late Tertiary eruptive centers.

Conclusions

The 20-Ma Burnett Inlet Igneous Complex in central southeastern Alaska consists of coeval granite and gabbro plutons that constitute a bimodal igneous complex. The within-plate characteristics of the felsic and mafic rocks relate the post-terrane accretionary magmatism within the Kuiu–Etolin Igneous Belt to the extensional tectonic regime documented in the neighboring Queen Charlotte Basin. Our model for the formation and differentiation of the Burnett Inlet Igneous Complex includes the following (see Fig. 15):

1. Tholeiitic mafic magma was generated by partial melting of enriched upper mantle *via* decompression-induced mantle melting in a tensional environment.
2. Mafic magma ponded at the base of the crust, causing partial melting of a source comprised of graywacke and intercalated volcanogenic material to generate mildly peraluminous A-type granite. Mafic and felsic magmas began to evolve at depth by fractional crystallization.
3. Mafic and felsic magmas rose through the lower and middle crust along post-Eocene extension-related fractures.
4. Mafic and felsic magmas were emplaced into the upper crust, where further fractional crystallization generated evolved types of magma. Differentiated magmas mixed and mingled, and were replenished with basaltic and granitic magmas. Intrusion of mafic magma into the felsic magma chamber caused superheating and convection of the granitic melt, enabling the entire magma suite to enter an eruptive phase.
5. The release of pressure by volcanic eruption led to rapid crystallization and cooling of the magma system.

Acknowledgements

This research was supported by grants in aid of research from Sigma Xi and the Geological Society of America to J. Lindline and National Science Foundation grant EAR–9304321 to M.L. Crawford. We thank A.K. Sinha for assistance in Rb–Sr isotope analysis, and K. Hollacher and G. Shaw for assistance with trace-element analysis. JL thanks E.A. Srogi and T. Lutz for helpful discussions on magma interactions, and D. Tuttle for assistance in the field. We thank B. Murphy, D.B. Clark and R.F. Martin for helpful reviews.

References

Barker, F. & Arth, J.G. (1990): Two traverses across the Coast batholith, southeastern Alaska. *Geol. Soc. Am., Mem.* **174**, 395-405.

Barbarin, B. (1988): Field evidence for successive mixing and mingling between Piolard diorite and the Saint-Julien-la-Vetre monzogranite (Nord-Forez, Massif Central, France). *Can. J. Earth Sci.* **25**, 49-59.

Berg, H.C., Jones, D.L. & Richter, D.H. (1972): Gravina–Nutzotin belt – tectonic significance of an upper Mesozoic sedimentary and volcanic sequence in southern and southeastern Alaska. *U.S. Geol. Surv., Prof. Pap.* **800-D**, D1-D24.

Black, R. & Girod, M. (1970): Late Palaeozoic to Recent igneous activity in West Africa and its relationship to basement structure. *In* African Magmatism and Tectonics (T.N. Clifford & I.G. Gass, eds.). Oliver and Boyd, Edinburgh, U.K. (185-210).

Bockelie, J.R. (1978): The Oslo region during the early Palaeozoic. *In* Tectonics and Geophysics of Continenal Rifts (I.B. Ramberg & E.-R. Neumann, eds.). *NATO Adv. Study Inst.* **C 37**. Reidel, Dordrecht, The Netherlands (195-202).

Brew, D.A. (1994): Latest Mesozoic and Cenozoic magmatism in southeastern Alaska. *In* The Geology of Alaska (G. Plafker & H.C. Berg, eds.). *Geol. Soc. Am., G–1*, 621-656.

_____, Berg, H.C., Morrell, R.P., Sonnevil, R.A, Hunt, S.J. & Huie, C. (1979): The mid-Tertiary Kuiu–Etolin volcanic-plutonic belt, southeastern Alaska. *In* The United States Geological Survey in Alaska: Accomplishments during 1978 (K.M. Johnson & J.R. Williams, eds.). *U.S. Geol. Surv., Circ.* **804-B**, 129-130.

_____ & Morrell, R.P. (1983): Intrusive rocks and plutonic belts in southeastern Alaska. *In* Circum-Pacific Plutonic Terranes (J.A. Roddick, ed.). *Geol. Soc. Am., Mem.* **159**, 171-193.

_____, Ovenshine, A.T., Karl, S.M. & Hunt, S.J. (1984): Preliminary reconnaissance geologic map of the Petersburg and parts of the Port Alexander and Sumdum 1:250,000 quadrangles, southeasten Alaska. *U.S. Geol. Surv., Open File Rep.* **84-405**.

_____, Sonnevil, R.A., Hunt, S.J. & Ford, A.B. (1981): Newly recognized alkali granite stock, southwestern Kupreanof Island, Alaska. *In* The United States Geologic Survey in Alaska: Accomplishments during 1979 (N.R.D. Albert & T. Hudson, eds.). *U.S. Geol. Surv., Circ.* **823-B**, 108-109.

Brotzu, P., Ganzerli-Valentini, M.T., Morbidelli, L., Piccirillo, E.M., Stella, R. & Traversa, G. (1981): Basaltic volcanism in the Northern sector of the main Ethiopian rift. *J. Volcanol. Geotherm. Res.* **10**, 365-382.

Carslaw, H.S. & Jaeger, J.C. (1959): *Conduction of Heat in Solids* (2nd ed.). Oxford University Press, Inc., New York, N.Y.

CHAPPELL, B.W. & WHITE, A.J.R. (1974): Two contrasting granite types. *Pac. Geol.* **8**, 173-174.

CLEMENS, J.D., HOLLOWAY, J.R., & WHITE, A.J.R. (1986): Origin of A-type granite: experimental constraints. *Am. Mineral.* **71**, 317-324.

CONEY, P.J. & JONES, D.L. (1985): Accretion tectonics and crustal structure in Alaska. *Tectonophys.* **119**, 265-283.

_____, _____ & MONGER, J.W.H. (1980): Cordilleran suspect terranes. *Nature* **288**, 329-333.

CONWAY, K.W., BARRIE, J.V. & ROHR, K.M.M. (1995): Neotectonics and surficial geology in Dixon entrance, British Columbia continental shelf. *Geol. Assoc. Can. – Mineral. Assoc. Can., Program Abstr.* **20**, A19.

COOK, R.D. (1991): *Mid-Cretaceous Granitoids and Orogeny in Southeasternmost Southeastern Alaska*. Ph.D. thesis, Bryn Mawr College, Bryn Mawr, Pennsylvania.

CRAWFORD, W.A., CRAWFORD, M.L. & SINHA, A.K. (1995): Evolutionary paths of members of the Late Cenozoic alkaline olivine basalt family of southeastern Alaska. *Geol. Assoc. Can. – Mineral. Assoc. Can., Program Abstr.* **20**, A21.

DIDIER, J. (1973): *Granites and their Enclaves*. Elsevier, New York, N.Y.

_____ & BARBARIN, B. (1991): *Enclaves and Granite Petrology*. Elsevier, Amsterdam, The Netherlands.

DOUGLASS, S.L., WEBSTER, J.H., BURRELL, P.D., LANPHERE, M.L. & BREW, D.A. (1989): Major-element chemistry, radiometric ages, and locations of samples from the Petersburg and parts of the Port Alexander and Sumdum quadrangles, southeastern Alaska. *U.S. Geol. Surv., Open File Rep.* **89- 527**.

DUGGAN, K. (1987): *Petrology of Metasediments in the Southeastern Corner of the Petersburg Quadrangle, Southeastern Alaska*. Senior thesis, Bryn Mawr College, Bryn Mawr, Pennsylvania.

ENGEBRETSON, D.C. (1989): Northeast Pacific – North America plate kinematics since 70 Ma. *Geol. Assoc. Can., Pacific Section, Annual* Symp. (*Victoria*), *Programme Abstr.*, 4-6.

_____, COX, A. & GORDON, R.G. (1985): Relative motions between oceanic and continental plates in the Pacific Basin. *Geol. Soc. Am., Spec. Pap.* **206**.

FEIGENSON, M.D. & CARR, M.J. (1985): Determination of major, trace and rare-earth elements by DCP–AES. *Chem. Geol.* **51**, 19-27.

FROST, T.P. & MAHOOD, G.A. (1987): Field, chemical and physical constraints on mafic–felsic magma interaction in the Lamark Granodiorite, Sierra Nevada, California. *Geol. Soc. Am., Bull.* **99**, 272-291.

FURMAN, T. & SPERA, F.J. (1985): Co-mingling of acid and basic magma with implications for the origin of I-type xenoliths: field and petrochemical relations of an unusual dike complex at Eagle Lake, Sequoia National Park, California, USA. *J. Volcanol. Geotherm. Res.* **24**, 151-178.

GEHRELS, G.E., MCCLELLAND, W.C., SAMSON, S.D., PATCHETT, P.J. & BREW, D.A. (1991): U–Pb geochronology of the Late Cretaceous and early Tertiary plutons in the northern Coast Mountains Batholith. *Can. J. Earth Sci.* **28**, 899-911.

GERDES, M. (1988): *P–T Constraints on Metamorphism of Metasediments in the Ketchikan and Petersburg Quadrangles, SE Alaska*. Senior thesis, Bryn Mawr College, Bryn Mawr, Pennsylvania.

GILBERT, M.C. (1983). Timing and chemistry of igneous events associated with the southern Oklahoma aulacogen. *Tectonophys.* **94**, 439-445.

_____ & DONOVAN, R.N. (1982): Geology of the eastern Wichita Mountains, southwestern Oklahoma. *Oklahoma Geol. Surv., Field Trip Guidebook* **21**.

GLEADOW, A.J.W. & BROOKS, C.K. (1979): Fission track dating, thermal histories and tectonics of igneous intrusions in East Greenland. *Contrib. Mineral. Petrol.* **71**, 45-60.

GREEN, P.F. (1981): A new look at statistics in fission track dating. *Nuclear Tracks* **5**, 77-86.

HARRISON, M.T., ARMSTRONG, R.L., NAESER, C.W. & HARAKAL, J.E. (1979): Geochronology and thermal history of the Coast Plutonic Complex, near Prince Rupert, British Columbia. *Can. J. Earth Sci.* **16**, 400-410.

_____ & CLARKE, G.K.C. (1979): A model of the thermal effects of igneous intrusion and uplift as applied to Quottoon pluton, British Columbia. *Can. J. Earth Sci.* **16**, 411-420.

_____ & MCDOUGALL, I. (1980): Investigations of an intrusive contact, northwest Nelson, New Zealand. I. Thermal, chronological and isotopic constraints. *Geochim. Cosmochim. Acta* **44**, 1985- 2003.

HIBBARD, M.J. (1981): The magma mixing origin of mantled feldspars. *Contrib. Mineral. Petrol.* **76**, 158-170.

_____ (1995): *Petrography to Petrogenesis*. Prentice Hall, Inc., Englewood Cliffs, New Jersey.

HUNT, S.J. (1984): Preliminary study of a zoned leucocratic-granite body on central Etolin Island, southeastern Alaska. *In* The United States Geological Survey in Alaska: Accomplishments during 1981 (W.L. Coonrad & R.L. Elliot, eds.). *U.S. Geol. Surv., Circ.* **868**, 128-131.

JONES, D.L., SILBERLING, N.J., BERG, H.C. & PLAFKER, G. (1981): Tectonostratigraphic terrane map of Alaska. *U.S. Geol. Surv., Open File Rep.* **81-792**.

KOCH, R.D., SMITH, J.G. & ELLIOT, R.L. (1977): Miocene or younger strike-slip(?) fault at Canoe Passage, southeastern Alaska. *In* Geological Studies in Alaska by the U.S. Geological Survey during 1976 (K.M. Blean, ed.). *U.S. Geol. Surv., Circ.* **751-B**, 76.

KYLE, P.R. (1981): The mineralogy and geochemistry of a basanite to phonolite sequence at Hut Point Peninsula, Antarctica, based on ore from the Dry Valley Drilling Project drillholes 1, 2 and 3. *J. Petrol.* **22**, 451-500.

LAMEYRE, J. & BOWDEN, P. (1982): Plutonic rock type series: discrimination of various granitoid series and related rocks. *J. Volcanol. Geotherm. Res.* **14**, 169-186.

LARSEN, E.S. (1945): Time required for the crystallization of the great batholith of southern and lower California. *Am. J. Sci.* **243A**, 399-416.

LEWIS, P.D., HAGGART, J.W., ANDERSON, R.G., HICKSON, C.J., THOMPSON, R.I., DIETRICH, J.R. & ROHR, K.M.M. (1991): Triassic to Neogene geologic evolution of the Queen Charlotte region. *Can. J. Earth Sci.* **28**, 854-869.

LINDLINE, J. (1993): *The Deer–Etolin Igneous Complex, Southeastern Alaska: a Study of Mingled and Mixed Magmas.* M.A. thesis, Bryn Mawr College, Bryn Mawr, Pennsylvania.

LOFGREN, G. (1980): Experimental studies on the dynamic crystallization of silicate melts. *In* Physics of Magmatic Processes (R.B. Hargraves, ed.). Princeton University Press, Princeton, New Jersey (487-551).

LONSDALE, P.F. (1988): Paleogene history of the Kula Plate: offshore evidence and onshore implications. *Geol. Soc. Am., Bull.* **100**, 733-754.

LULL, J.S. & PLAFKER, G. (1988): Geochemistry and petrography of lamprophyre dike rocks in the Coast Mountains, southeastern Alaska. *In* Geologic Studies in Alaska by the U.S. Geological Survey in 1987 (J.P. Galloway & T.D. Hamilton, eds.). *U.S. Geol. Surv., Circ.* **1016**, 169-173.

MAALØE, S. & WYLLIE, P.J. (1975): Water content of a granite magma deduced from the sequence of crystallization determined experimentally with water-undersaturated conditions. *Contrib. Mineral. Petrol.* **52**, 175-191.

MANIAR, P.D. & PICCOLI, P.M. (1989): Tectonic discrimination of granitoids. *Geol. Soc. Am., Bull.* **101**, 635-643.

MCBIRNEY, A.R. (1980): Mixing and unmixing of magmas. *J. Volcanol. Geotherm. Res.* **7**, 357-371.

MONGER, J.W.H., PRICE, R.A. & TEMPELMAN-KLUIT, D.J. (1982): Tectonic accretion and the origin of two major metamorphic and plutonic welts in the Canadian Cordillera. *Geology* **10**, 70-75.

NAESER, C.W. (1976): Fission track dating. *U.S. Geol. Surv., Open File Rep.* **76-190**.

NAKAMURA, N. (1974): Determination of REE, Ba, Fe, Mg, Na and K in carbonaceous and ordinary chondrites. *Geochim. Cosmochim. Acta* **38**, 757-775.

NANEY, M.T. (1983): Phase equilibria of rock-forming ferromagnesian silicates in granitic systems. *Am. J. Sci.* **283**, 993-1033.

OMAR, G.I., KOHN, B.P., LUTZ, T.M. & FAUL, H. (1987): The cooling history of Silurian to Cretaceous alkaline ring complexes, south Eastern Desert, Egypt, as revealed by fission-track analysis. *Earth Planet. Sci. Lett.* **83**, 94-108.

PARRISH, R.R. (1983): Cenozoic thermal evolution and tectonics of the Coast Mountains of British Columbia. 1. Fission track dating, apparent uplift rates, and patterns of uplift. *Tectonics* **2**, 601-631.

PEARCE, J.A. (1983): Role of sub-continental lithosphere in magma genesis at active continental margins. *In* Continental Basalts and Mantle Xenoliths (C.J. Hawkesworth & M.J. Norry, eds.). Shiva Press, Nantwich, U.K. (230-249).

_____, HARRIS, N.B.W. & TINDLE, A.G. (1984): Trace element discrimination diagrams for the tectonic interpretation of granitic rocks. *J. Petrol.* **25**, 956-983.

ROHR, K.M.M. & FURLONG, K.P. (1995): Uplift and subsidence as the response to a change to transpression on the Queen Charlotte Fault. *Geol. Assoc. Can. – Mineral. Assoc. Can., Program Abstr.* **20**, A90.

ROLLINSON, H.R. (1993): *Using Geochemical Data: Evaluation, Presentation, Interpretation*. J. Wiley and Sons, New York, N.Y.

RUTTER, M.J. & WYLLIE, P.J. (1988): Melting of vapor-absent tonalite at 10 kbar to simulate dehydration-melting in the deep crust. *Nature* **331**, 159-160.

SHAW, D.M. (1970): Trace element fractionation during anatexis. *Geochim. Cosmochim. Acta* **34**, 237-243.

SHERVAIS, J.W. (1982): Ti–V plots and the petrogenesis of modern and ophiolitic lavas. *Earth Planet. Sci. Lett.* **59**, 101-118.

SKJERLIE, K.P. & JOHNSTON, A.D. (1992): Vapor-absent melting at 10 kbar of a biotite- and amphibole-bearing tonalitic gneiss: implications for the generation of A-type granites. *Geology* **20**, 263-266.

SMITH, J.G. (1973): A Tertiary lamprophyre dike province in southeastern Alaska. *Can. J. Earth Sci.* **10**, 408-420.

SPARKS, S.R.J., SIGURDSSON, H. & WILSON, L. (1977): Magma mixing: a mechanism for triggering acid explosive eruptions. *Nature* **267**, 315-318.

STOCK, J. & MOLNAR, P. (1988): Uncertainties and implications of Late Cretaceous and Tertiary positions of the North America plate relative to the Farallon, Kula and Pacific plates. *Tectonophys.* **7**, 1339-1384.

STRECKEISEN, A. (1978): IUGS subcommission on the systematics of igneous rocks. Classification and nomenclature of volcanic rocks, lamprophyres, carbonatites and melilite rocks. Recommendations and suggestions. *Neues Jahrb. Mineral., Abh.* **143**, 1-14.

VERNON, R.H. (1983): Restite, xenoliths, and microgranitoid enclaves in granites. *J. Proc. R. Soc. New South Wales* **116**, 77-103.

_____ (1984): Microgranitoid enclaves in granites: globules of hybrid magma quenched in a plutonic environment. *Nature* **304**, 438-439.

_____ (1990): Crystallization and hybridism in microgranitoid enclave magmas: microstructural evidence. *J. Geophys. Res.* **95**, 17,849-17,859.

VIELZEUF, D. & MONTEL, J.M. (1994): Partial melting of metagreywackes. I. Fluid-absent experiments and phase relationships. *Contrib. Mineral. Petrol.* **117**, 375-393.

WHALEN, J.B., CURRIE, K.L. & CHAPPELL, B.W. (1987): A-type granites: geochemical characteristics, discrimination and petrogenesis. *Contrib. Mineral. Petrol.* **95**, 407-419.

WHEELER, J.O., BROOKFIELD, A.J., GABRIELSE, H., MONGER, J.W.H., TIPPER, T.W. & WOODSWORTH, G.J. (1991): Terrane map of the Canadian Cordillera. *Geol. Surv. Can., Open File Rep.* **1894**.

WHITE, A.J.R. & CHAPPELL, B.W. (1983): Granitoid types and their distribution in the Lachland fold belt, southeastern Australia. *Geol. Soc. Am., Mem.* **159**, 21-34.

WYLLIE, P.J. (1977): Crustal anatexis: an experimental review. *Tectonophys.* **43**, 41-71.

_____ (1984): Constraints imposed by experimental petrology on possible and impossible magma sources and products. *R. Soc. London Philos. Trans.* **A310**, 439-456.

_____, COX, K.G. & BIGGAR, G.M. (1962): The habit of apatite in synthetic systems and igneous rocks. *J. Petrol.* **3**, 238-242.

YORK, D. (1969): Least squares fitting of a straight line with correlated errors. *Earth Planet. Sci. Lett.* **5**, 320-324.

ZEITLER, P.K. (1985): Cooling history of the NW Himalaya, Pakistan. *Tectonics* **4**, 127-151.

Received June 15, 1999, revised manuscript accepted May 23, 2000.